AD-A111 758 NAVAL POSTGRADUATE SCHOOL MONTEREY CA F/G 20/11
A STUDY OF NOTCH FATIGUE. PART III. PLASTIC STRESS ANALYSIS OF --ETC(U)
SEP 81 G H LINDSEY
UNCLASSIFIED NPS67-81-006 NL

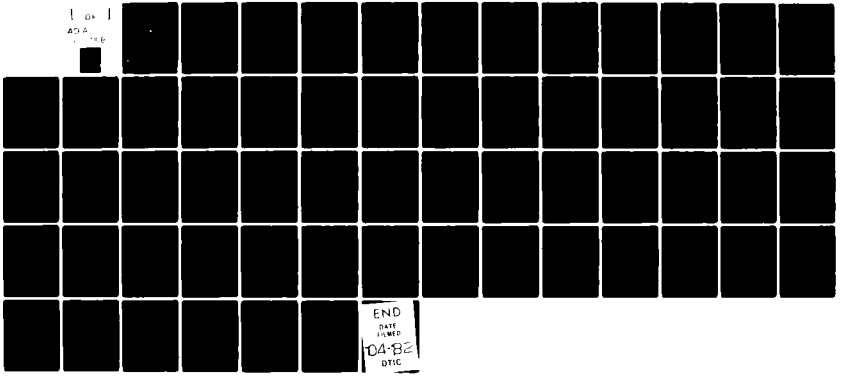

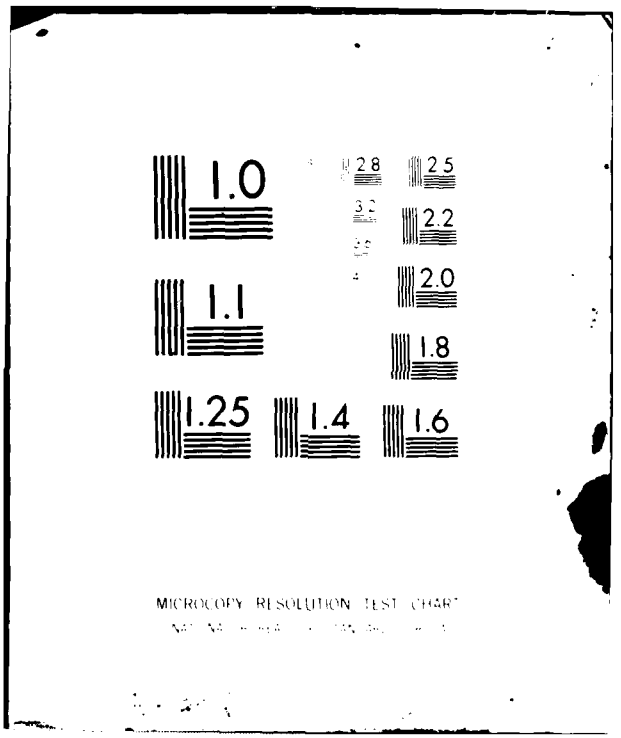
1.0
2.8
2.5
2.2
2.0
1.1
1.8
1.25
1.4
1.6
MICROCOPY RESOLUTION TEST CHART

NPS67-81-006

(2)

NAVAL POSTGRADUATE SCHOOL
Monterey, California

A STUDY OF NOTCH FATIGUE

PART III: PLASTIC STRESS ANALYSIS OF NOTCHES

GERALD H. LINDSEY

September 1981

Prepared for:
Naval Air Systems Command
Washington, DC 20361

Naval Postgraduate School
Monterey, California

Rear Admiral J. J. Ekelund
Superintendent

D. A. Schrady
Acting Provost

The work reported herein was supported by the Naval Air Systems Command, Washington, DC.

This report was prepared by:

GERALD H. LINDSEY
Professor of Aeronautics

Reviewed by:

M. F. PLATZER
Chairman of Aeronautics

Released by:

W. M. TOLLES
Dean of Research

UNCLASSIFIED
SECURITY CLASSIFICATION OF THIS PAGE (When Data Entered)

REPORT DOCUMENTATION PAGE		READ INSTRUCTIONS BEFORE COMPLETING FORM
1. REPORT NUMBER NPS67-81-006	2. GOVT ACCESSION NO.	3. RECIPIENT'S CATALOG NUMBER
4. TITLE (and Subtitle) A Study of Notch Fatigue Part III: Plastic Stress Analysis of Notches		5. TYPE OF REPORT & PERIOD COVERED PROGRESS REPORT Oct 1980 - Sept 1981 6. PERFORMING ORG. REPORT NUMBER
7. AUTHOR(s) Gerald H. Lindsey		8. CONTRACT OR GRANT NUMBER(s)
9. PERFORMING ORGANIZATION NAME AND ADDRESS Naval Postgraduate School Monterey, CA 93940		10. PROGRAM ELEMENT, PROJECT, TASK AREA & WORK UNIT NUMBERS 61153N N0001981WR11104
11. CONTROLLING OFFICE NAME AND ADDRESS Naval Air Systems Command Washington, DC 20361		12. REPORT DATE SEPTEMBER 1981 13. NUMBER OF PAGES
14. MONITORING AGENCY NAME & ADDRESS(if different from Controlling Office)		15. SECURITY CLASS. (of this report) UNCLASSIFIED 15a. DECLASSIFICATION/DOWNGRADING SCHEDULE

16. DISTRIBUTION STATEMENT (of this Report)

Approved for Public; distribution unlimited.
RELEASE

17. DISTRIBUTION STATEMENT (of the abstract entered in Block 20, if different from Report)

18. SUPPLEMENTARY NOTES

19. KEY WORDS (Continue on reverse side if necessary and identify by block number)

Notch, Plastic yielding, stress concentration factor, Residual stress, Residual strain

20. ABSTRACT (Continue on reverse side if necessary and identify by block number)

The stress and strain behavior at notch tips is analyzed with the view of using local values for fatigue calculations. A perfectly plastic, closed form solution is used as a starting point and basis of comparison for the finite element analysis. Maximum stress and strain values for 7075-T6 aluminum were obtained via finite elements and reflection photoelasticity in the plastic zone, and residual stress and strain values after unloading were obtained as well. A uniaxial model was used successfully to predict most of the behavior observed.

DD FORM 1 JAN 73 1473 EDITION OF 1 NOV 65 IS OBSOLETE
S/N 0102-014-6601

UNCLASSIFIED
SECURITY CLASSIFICATION OF THIS PAGE (When Data Entered)

Table of Contents

ABSTRACT

The stress and strain behavior at notch tips is analyzed with the view of using local values for fatigue calculations. A perfectly plastic, closed form solution is used as a starting point and basis of comparison for the finite element analysis. Maximum stress and strain values for 7075-T6 aluminum were obtained via finite elements and reflection photoelasticity in the plastic zone, and residual stress and strain values after unloading were obtained as well. A uniaxial model was used successfully to predict most of the behavior observed.

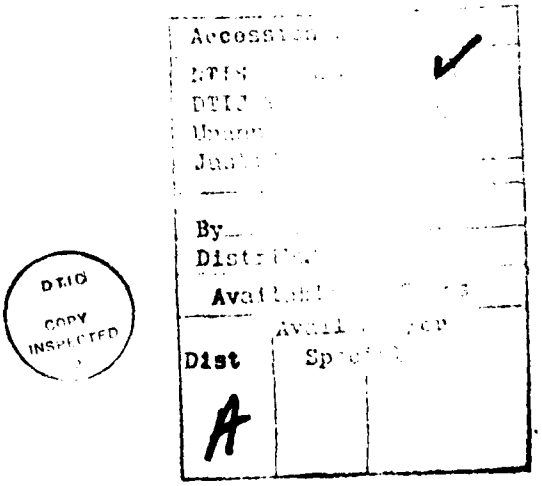

A STUDY OF NOTCH FATIGUE

PART III: PLASTIC STRESS ANALYSIS OF NOTCHES

INTRODUCTION

As aircraft maneuver through a varied and complicated load history, critical points at sites of stress concentration are locally loaded into the plastic range. This is a good protection factor for the structure, for the yielding provides a large load bearing capability for loads beyond the limit load. However, yielding at the fatigue critical points also greatly influences the fatigue life of the part, and calculations of fatigue must include these effects in order to be accurate.

RESIDUAL STRESS

After a load cycle is applied which takes the ligaments at the notch tip into the yield zone, those ligaments have a permanent set, which makes them longer than their original length. During the unloading portion of the cycle, the surrounding unyielded material attempts to push the elongated ligaments back to their original length and a position of equilibrium is attained with the ligaments in compression; thus, a compressive residual stress is produced in the ligaments. The ligaments are still longer than they were in the unyielded state and the notch tip region possesses a zone of compressive residual stress but positive residual strain. Both of these must be accounted for in a cycle by cycle summation of damage for fatigue life monitoring.

STRESS CONCENTRATION FACTOR

Tensile yielding at the notch tip causes a reduction in the stress concentration factor. Thinking of the ligament at

the notch tip as a miniature uniaxial tensile specimen, as the stress-strain curve for the ligament bends over with yielding, the ratio of far-field stress to the local plastic stress produced is larger than for the elastic condition and this relationship reduces the SCF. This change in SCF can have significant effect on fatigue life predictions for those cycles applied after a cycle which causes yielding.

PHOTOELASTIC RAMIFICATIONS

After yielding occurs in the specimen material, stresses and strains in the coating material undergo a shift relative to one another because the coating strains are constrained to be the same as the yielded metal so that the classical relationships for stress in terms of fringe number no longer hold. In this report strains are obtained photoelastically, and the stresses are calculated using plastic stress-strain laws. The coating, however, acts as a permanent repository of the residual strain for whatever loading may follow. To obtain the stresses, a model must be formulated, which gives the new stress-strain relation, where the zero stress point doesn't coincide any longer with the zero strain point but the two have been shifted apart.

All three of these phenomena will be explored in detail in this report with supporting experimental data to quantify the behavior.

PLANE STRESS SLIPLINE THEORY

To begin exploration into the nonlinear domain, some analytical methods were first searched for, and the only candidate seemed to be slipline theory. The material model is highly

idealized, but with photoelasticity and FEA, it is possible to assess its usefulness. It is an elegant theory, and it proved very useful in checking out the nonlinear portion of the ADINA Program. The development here follows that given by Kachnov[1].

GOVERNING EQUATIONS

In the plastic region, slipline theory assumes that the stress state is on the original yield surface, or in other words, that the material is perfectly plastic. Using the Von Mises yield criterion, this requires that

$$\sigma_1^2 - \sigma_1\sigma_2 + \sigma_2^2 = 3k^2 \qquad (1)$$

where k = yield limit in pure shear. The uniaxial yield stress is $\sigma_y = \sqrt{3}\,k$. A parametric form of this equation was developed by Sokolovskii,

$$\sigma_1 = 2k\,\mathrm{Cos}\left(\omega - \frac{\pi}{6}\right) \qquad \sigma_2 = 2k\,\mathrm{Cos}\left(\omega + \frac{\pi}{6}\right) \qquad (2)$$

which satisfies (1) identically for all values of ω.
The parametric function $\omega(x,y)$ is related to the mean pressure, which is given by

$$\sigma = \frac{1}{3}\left(\sigma_1 + \sigma_2 + \sigma_3\right) \qquad (3)$$

Substituting Equation (2) into Equation (3) and setting $\sigma_3 = 0$ for plane stress, we find

$$\mathrm{Cos}\,\omega = \frac{\sqrt{3}\,\sigma}{2k} \qquad (4)$$

To obtain the expression for equilibrium equations in terms of ω, the transformation equations are first used

$$\sigma_x = \frac{1}{2}(\sigma_1 + \sigma_2) + \frac{1}{2}(\sigma_1 - \sigma_2)\cos 2\phi \tag{5a}$$

$$\sigma_y = \frac{1}{2}(\sigma_1 + \sigma_2) - \frac{1}{2}(\sigma_1 - \sigma_2)\cos 2\phi \tag{5b}$$

$$\tau_{xy} = \frac{1}{2}(\sigma_1 - \sigma_2)\sin 2\phi \tag{5c}$$

where ϕ is the angle between the first principal direction and the x axis.

Substituting Equations (2) into (5),

$$\sigma_x = k\left[\sqrt{3}\cos\omega + \sin\omega\cos 2\phi\right] \tag{6a}$$

$$\sigma_y = k\left[\sqrt{3}\cos\omega - \sin\omega\cos 2\phi\right] \tag{6b}$$

$$\tau_{xy} = k\sin\omega\sin 2\phi \tag{6c}$$

Substituting the stress components into the differential equations of equilibrium simplified to plane stress, we obtain a system of two equations for the two unknown functions $\omega(x,y)$ and $\phi(x,y)$. After some rearrangement to simplify later operations, the two equations become

$$(\sqrt{3}\sin\omega\cos 2\phi - \cos\omega)\frac{\partial\omega}{\partial x} + \sqrt{3}\sin\omega\sin 2\phi\frac{\partial\omega}{\partial y} - 2\sin\omega\frac{\partial\phi}{\partial y} = 0 \tag{7a}$$

$$(\sqrt{3}\sin\omega\sin 2\phi)\frac{\partial\omega}{\partial x} - (\sqrt{3}\sin\omega\cos 2\phi + \cos\omega)\frac{\partial\omega}{\partial y} + 2\sin\omega\frac{\partial\phi}{\partial x} = 0 \tag{7b}$$

METHOD OF CHARACTERISTICS

Seeking a solution by the method of characteristics, we suppose that along some line in the structure given by $x = x(s)$ and $y = y(s)$, the functions $\omega = \omega(s)$ and $\phi = \phi(s)$ are given. Then along that line

$$\frac{d\phi}{ds} = \frac{\partial \phi}{\partial x}\frac{dx}{ds} + \frac{\partial \phi}{\partial y}\frac{dy}{ds} \tag{8a}$$

$$\frac{d\omega}{ds} = \frac{\partial \omega}{\partial x}\frac{dx}{ds} + \frac{\partial \omega}{\partial y}\frac{dy}{ds} \tag{8b}$$

Equations (7) and (8) possess characteristics whose defining differential equations are found by setting the determinant of the coefficients to zero. Reducing the determinant we obtain

$$\frac{dy}{dx} = \frac{\sqrt{3}\sin\omega \sin 2\phi \pm \sqrt{3-4\cos^2\omega}}{\sqrt{3}\sin\omega\cos 2\phi - \cos\omega} \tag{9}$$

In order for the characteristics to be real, the discriminant must be positive semi definite,

$$3-4\cos^2\omega \geq 0 \tag{10}$$

or

$$\omega \geq \frac{\pi}{6}$$

Therefore, because of the nature of the cosine function, the region of hyperbolic characteristics lies between the limits $\frac{\pi}{6} \leq \omega \leq \frac{5\pi}{6}$. From Equation (10)

$$\cos\omega \leq \frac{\sqrt{3}}{2} \tag{11}$$

and from Equation (4) we see that this physically corresponds to

$$\sigma \leq k \tag{12}$$

which means that the mean pressure must be less than the maximum shear stress in order to have a region where the equations are hyperbolic and characteristics exist.

In the application of Kramer's Rule to solve the set of simultaneous equations for $\frac{dx}{ds}$, a numerator determinant is formed. Setting this determinant to zero gives the condition along one set of characteristics, which reduces to

$$\Omega + \phi = \text{Constant} \tag{13}$$

where

$$\Omega = -\frac{1}{2}\int_{\frac{\pi}{6}}^{\omega} \frac{\sqrt{3-4\cos^2\omega}}{\sin\omega}\, d\omega \tag{14}$$

Along the other set of characteristics, obtained by setting the determinant for $\frac{dy}{ds} = 0$, we find

$$\Omega - \phi = \text{Constant} \tag{15}$$

CIRCULAR BOUNDARIES

Consider a portion of a circular boundary as shown in Figure 1.

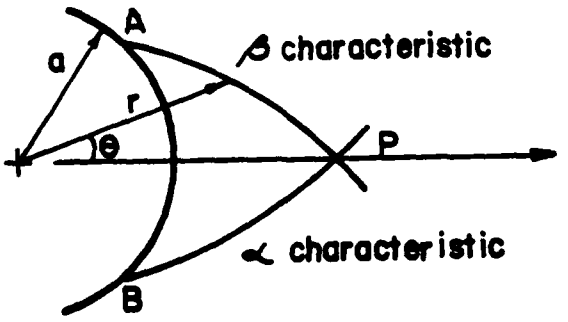

FIGURE 1 SCHEMATIC OF CHARACTERISTICS

Stress conditions at point P will only be influenced by conditions along the portion of the boundary between A and B, and if the boundary changes contour outside of AB it will not affect the stresses at P. More specifically, the stresses at P for a notch and for an axisymmetric hole would be the same, so long as all of the material between A and B were yielded and the boundary is stress free. At $r = a$ all along the yielded boundary, $\tau_{r\theta} = 0$ and $\sigma_r = 0$. By the Von Mises yield condition in Equation (1), $\sigma_\theta = \sqrt{3}k$; the mean pressure is $\sigma = \frac{k}{\sqrt{3}}$; and the maximum shear stress is $\tau_{max} = \frac{\sqrt{3}}{2}k$; thus, the condition is satisfied for characteristics. From Equation (4) $\omega = \frac{\pi}{3}$ at the boundary $r = a$.

From Equation (2) the normal stresses in the yielded region are given by

$$\sigma_r = 2k \cos\left(\omega + \frac{\pi}{6}\right) \tag{16a}$$

$$\sigma_\theta = 2k \cos\left(\omega - \frac{\pi}{6}\right) \tag{16b}$$

STRESS DISTRIBUTIONS

To relate ω to r, the axisymmetric form of the equilibrium equations is used.

$$\frac{d\sigma_r}{dr} + \frac{\sigma_r - \sigma_\theta}{r} = 0 \tag{17}$$

Substituting Equations (16) into (17) and simplifying, a relation between ω and r is obtained.

$$(\sqrt{3} + \cot\omega)d\omega + 2\frac{dr}{r} = 0 \tag{18}$$

Integrating,

$$r^2 = \frac{C}{\sin\omega} e^{-\sqrt{3}\omega} \tag{19}$$

where C is a constant of integration.

As shown before, on the boundary at $r = a$, $\omega = \frac{\pi}{3}$. Using this point to evaluate C.

$$C = a^2 \frac{\sqrt{3}}{2} e^{\pi/\sqrt{3}} \tag{20}$$

and

$$r = \left[\frac{\sqrt{3}}{2} \frac{e^{\sqrt{3}\left(\frac{\pi}{3} - \omega\right)}}{\sin\omega}\right]^{\frac{1}{2}} a \tag{21}$$

Characteristics will extend out into the body to $\omega = \frac{\pi}{6}$, which corresponds to $r = 2.07a$. Within that region this solution will apply to the notch.

Equation (21) has been evaluated for the notch in Figure 2 given by $r = 1.8125$ in. and $d = 2.875$ in. out to a distance of $r = 3.75$ in., which corresponds to the limit of applicability of the solution. The results are listed in Table I.

The domain of applicability of the solution is defined by the free boundary at the edge of the notch and the two characteristics given by Equations (13) and (15). Since the solution for the notch coincides with the axisymmetric solution in this range, σ_r and σ_θ are principal stresses and $\phi = \theta$. Thus,

$$\Omega \pm \Theta = \text{Constant} \tag{22}$$

LARGE SPECIMEN GEOMETRIES

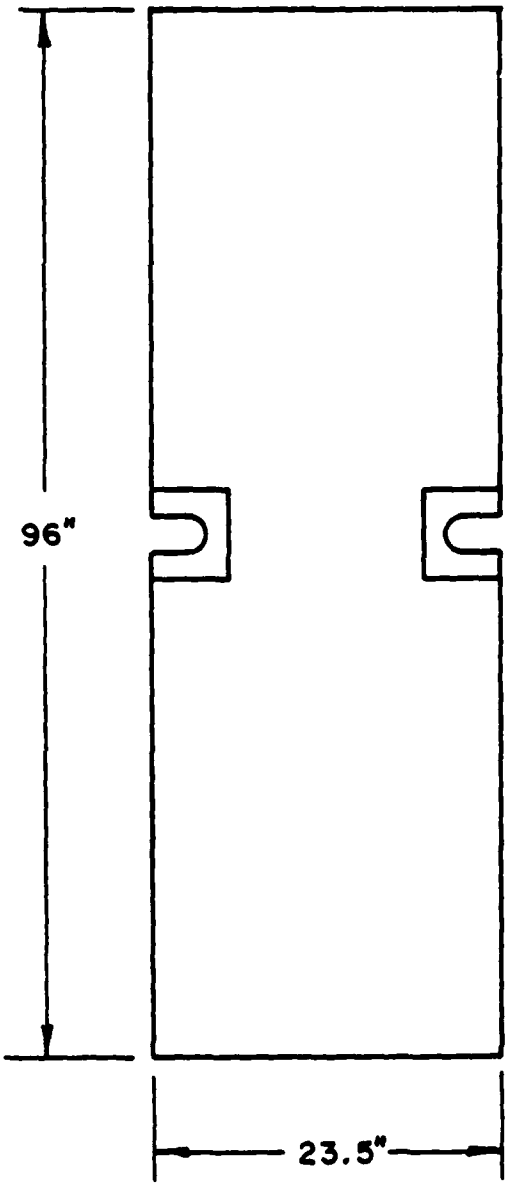

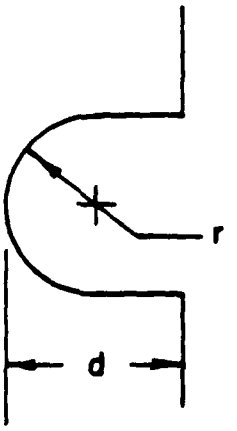

Nominal K_T	2.6	3.8
r (in)	1.8125	0.625
d (in)	2.875	3.938
Reduced Cross-section (in^2)	1.42 in^2	1.25 in^2

7075-T6 Aluminum
Thickness 0.080 in

FIGURE 2. NOTCH GEOMETRY

TABLE I

NOTCH STRESS DISTRIBUTION BY SLIPLINE THEORY

r	r/a	ω	$\sigma_r/\sqrt{3k}$	$\sigma_\theta/\sqrt{3k}$
1.8125	1.0000	$\pi/3$ = 1.047	0.0000	1.0000
2.1645	1.1942	$\pi/3.49$ = .900	0.1689	1.0740
2.4698	1.3626	$\pi/3.93$ = .799	0.2832	1.1113
2.8381	1.5658	$\pi/4.49$ .700	0.3925	1.1369
3.3057	1.8238	$\pi/5.24$ .600	0.4989	1.1514
3.7506	2.0690	$\pi/6$ .524	0.5774	1.1547

At the outer extremity of the zone, where $\omega = \pi/6$ and $r = 3.7506$, the characteristics intersect and coincide. From the definition of Ω given in Equation (14), it is zero at $\omega = \pi/6$ for all θ. Concerning ourselves with the point P in Figure 1, which corresponds to the symmetry line of the notch where $\theta = 0$, Equation (22) yields the value of the constant as zero. We therefore are looking for the characteristics defined by

$$\Omega \pm \Theta = 0 \tag{23}$$

Evaluating Ω from Equation (14) by Simpson's rule at all of the r values in Table I, and obtaining the corresponding θ coordinates from Equation (23), the trajectory of the characteristics can be found. They have been tabulated in Table II.

A plot of these contours has been made on the tip of the notch in Figure 3. This is not a drawing of the plastic zone, but is the boundary of applicability of the slipline solution.

This slipline method provides about the only analytical means of handling the nonlinear, plastic flow at a notch tip. Although it is limited to rigid, perfectly plastic material models and the extent of yielding is unknown; it does constitute a valid check on the FEA and later these results will be compared to those attained for more realistic material models.

COMPARISON WITH FEA

The finite element grid used for the elastic analysis reported in Part II[2] was employed with ADINA's bilinear material model such that it represented a rigid perfectly plastic material. A Young's Modulus of 10^{26} psi was used to model perfect

TABLE II

COORDINATES OF BOUNDING CHARACTERISTICS

r	w	θ
1.8125	1.047	$\pm$ 24.1°
2.1645	0.900	$\pm$ 17.3°
2.4698	0.799	$\pm$ 12.7°
2.8381	0.700	$\pm$ 8.1°
3.3057	0.600	$\pm$ 3.5°
3.7506	0.524	0°

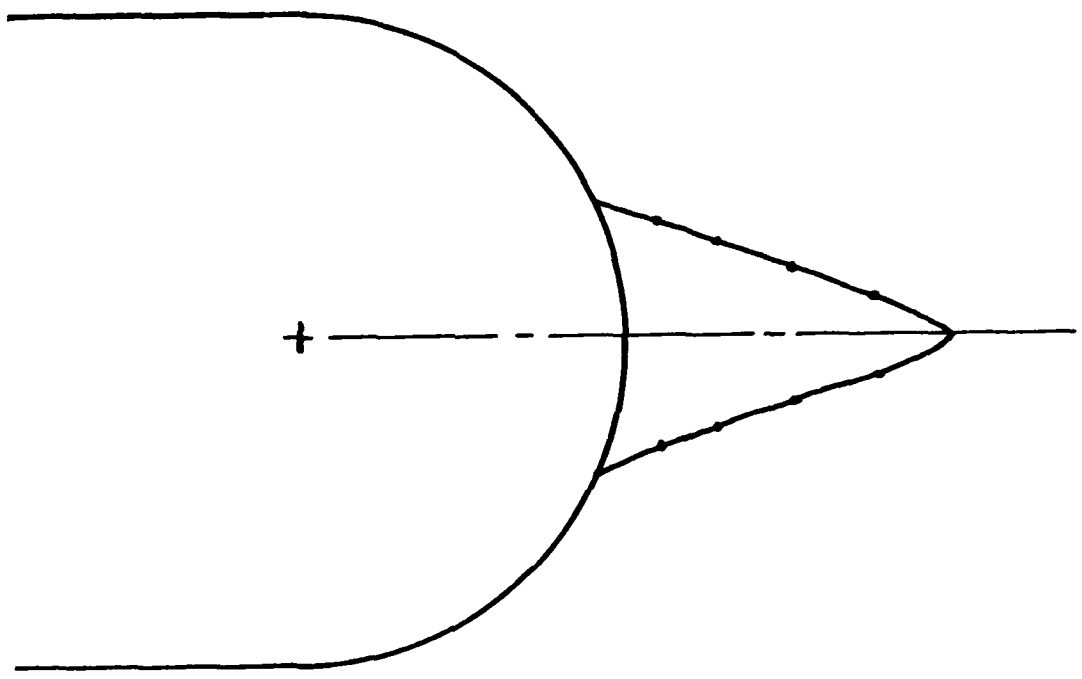

FIGURE 3. APPLICABLE REGION SLIPLINE SOLUTION

rigidity, and the strain hardening modulus, E_t , was set equal to zero. Poisson's ratio was entered as 0.4999999, which is as close to incompressibility as the program would allow.

Figure 4 illustrates the FEA results obtained and compares them to the slipline solution. The stress values are normalized to the yield stress. Very good correlation was obtained for the σ_θ distribution but the σ_r values vary somewhat. This seems to be par for this problem in that it seems no matter what method is used to find the stresses, the greater variation is always in σ_r . The comparisons are viewed, however, as substantiations of one another and constitute a baseline to which other analyses can be referenced.

The growth of the plastic zone, which is not obtainable in the slipline theory, is given by FEA in Figures 5 to 7.

We now explore a more realistic material model with FEA and with photoelasticity. In order to do that, it is necessary to develop a nonlinear stress-strain law.

PLASTIC STRESS-STRAIN RELATIONSHIP

When the proportional limit is exceeded at the notch tip, stresses can no longer be computed directly from the photoelastic fringe data. A plastic stress-strain relationship must be used to calculate stresses from measured strain values. From Druckers's Postulate[3] it has been shown that the plastic strain increment is normal to the yield function in stress ; i.e.

$$d\varepsilon_{ij}^{p} = \frac{\partial f}{\partial \sigma_{ij}} d\lambda \qquad (24)$$

FIGURE 4

RIGID-PERFECTLY-PLASTIC RESULTS

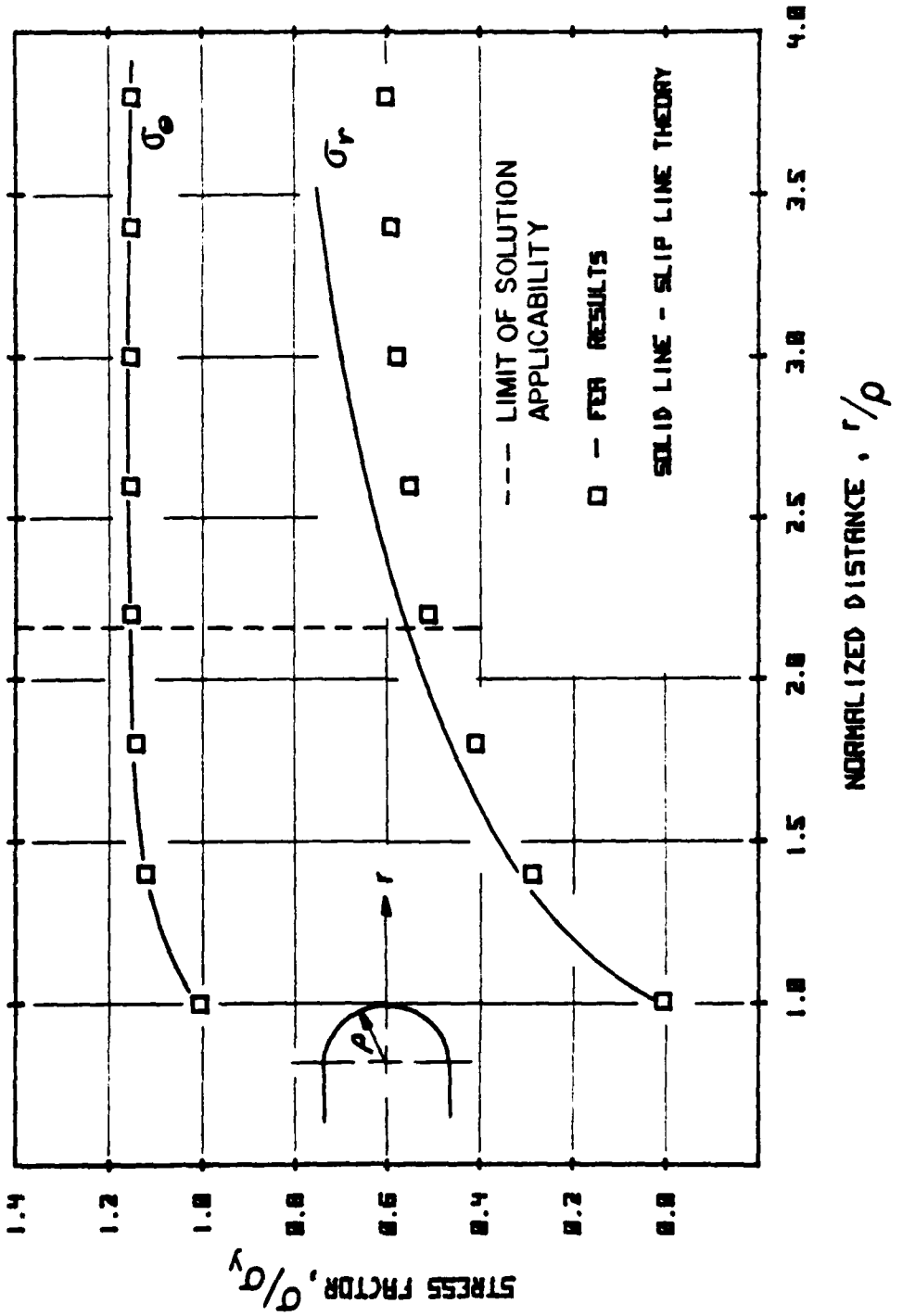

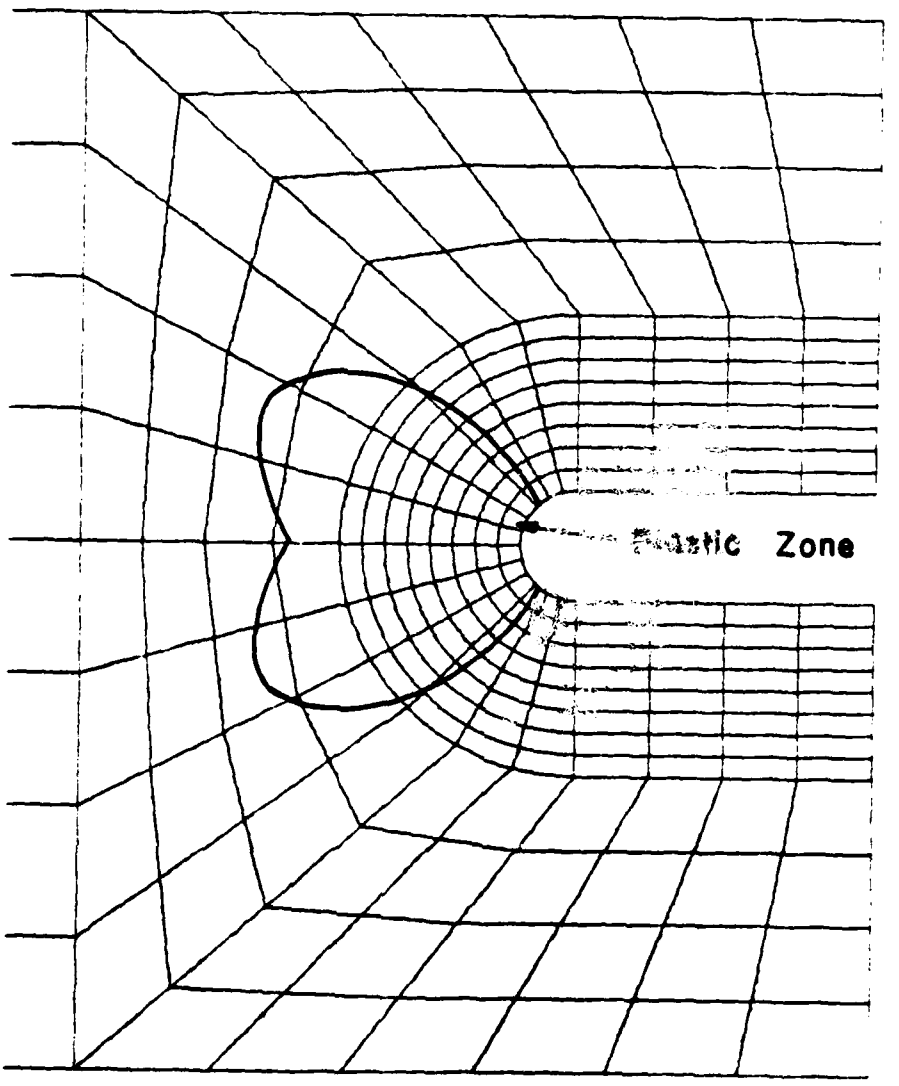

FIGURE 5

RIGID-PERFECTLY-PLASTIC INITIAL PLASTIC ZONE

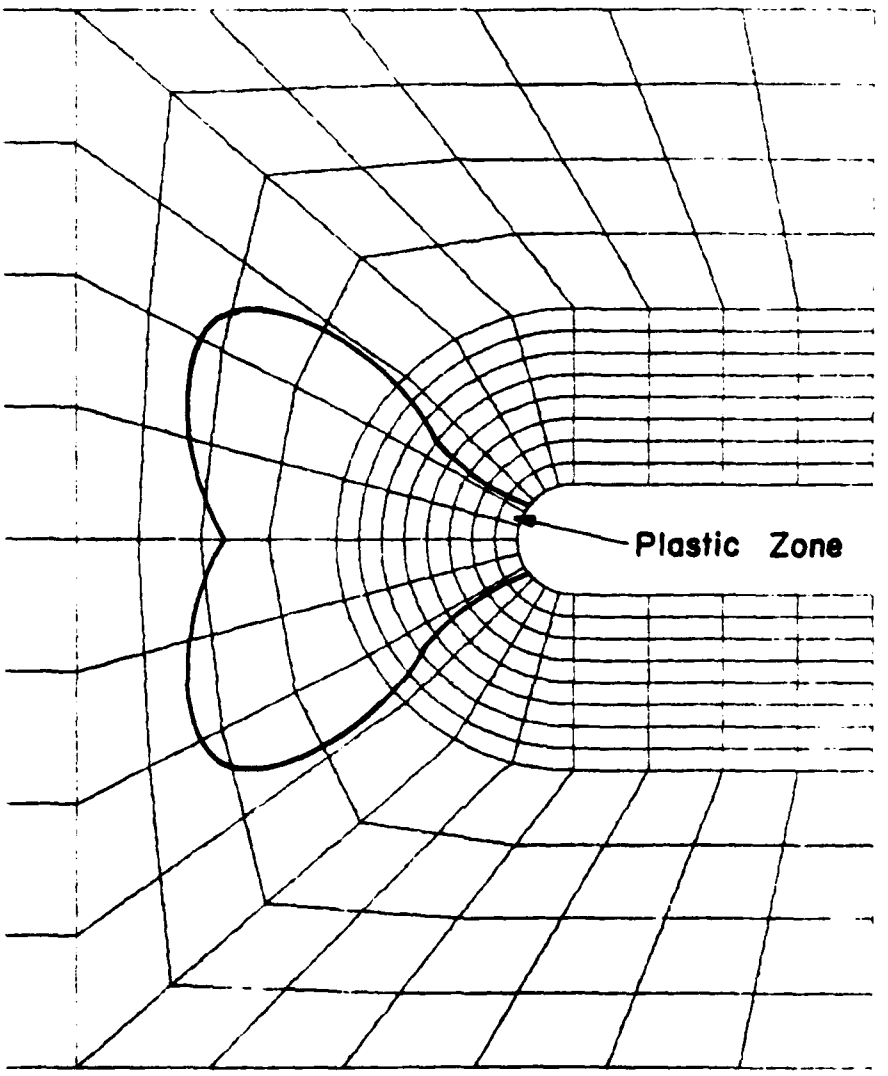

FIGURE 6

RIGID-PERFECTLY-PLASTIC INTERMEDIATE PLASTIC ZONE

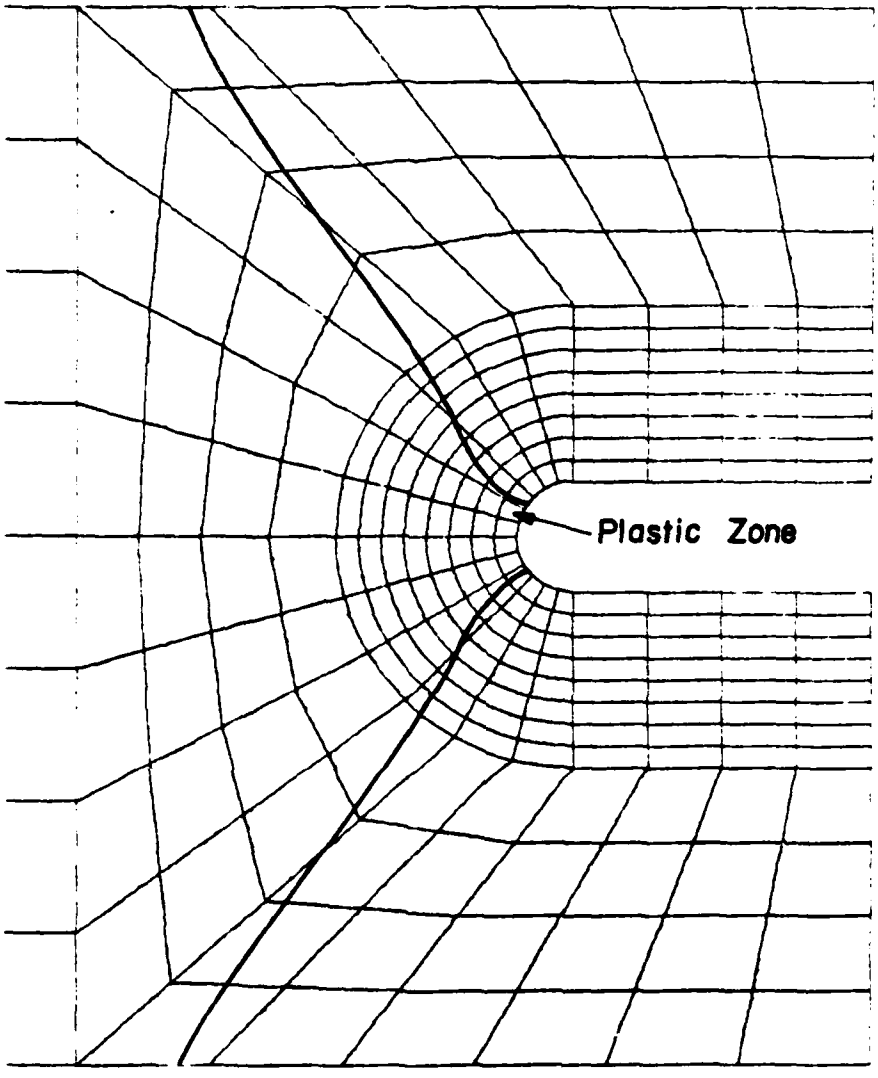

FIGURE 7

RIGID-PERFECTLY-PLASTIC FINAL PLASTIC ZONE

where $d\varepsilon ij^p$ = Plastic strain increment

$f(\sigma ij)$ = 0 describes the yield function

$d\lambda$ = An undetermined function of stress, strain and history of loading.

The Von Mises, or distortional energy, yield criterion is good for aluminum. In terms of principal stress invariants, yielding occurs when J_2 reaches a given value.

$$J_2 = \frac{1}{6}\left[(\sigma_1-\sigma_2)^2+(\sigma_2-\sigma_3)^2+(\sigma_1-\sigma_3)^2\right] = \text{Constant} \qquad (25)$$

where J_2 = Second deviatoric stress invariant

σ_i = Principal Stresses

The f is defined as

$$f(\sigma_i) = J_2 - \text{Constant} \qquad (26)$$

Differentiating as indicated in Equation (24).

$$d\varepsilon_1^p = \frac{2}{3}\left[\sigma_1 - \frac{1}{2}(\sigma_2+\sigma_3)\right]d\lambda \qquad (27a)$$

$$d\varepsilon_2^p = \frac{2}{3}\left[\sigma_2 - \frac{1}{2}(\sigma_1+\sigma_3)\right]d\lambda \qquad (27b)$$

$$d\varepsilon_3^p = \frac{2}{3}\left[\sigma_3 - \frac{1}{2}(\sigma_2+\sigma_1)\right]d\lambda \qquad (27c)$$

To determine $d\lambda$, an equivalent uniaxial stress, σ^*, is defined to represent the behavior of a triaxial stress state with a single component.

$$\sigma^* \equiv F(\sigma_1, \sigma_2, \sigma_3) \tag{28}$$

such that in uniaxial tension,

$$F(\sigma_1, 0, 0) = \sigma_1 \tag{29}$$

and at yield when $f = 0$

$$\sigma^* = \sigma_y \tag{30}$$

when $f = 0$, $J_2 = \text{Const}$, so it is convenient to let

$$\sigma^* \equiv F(J_2) \tag{31}$$

The simplest function is customarily selected.

$$\sigma^* = A J_2^{1/2} \tag{32}$$

where the square root is chosen to make the expression dimensionally correct. For uniaxial tension,

$$F(\sigma_1, 0, 0) = \frac{A}{\sqrt{6}} \left[2\sigma_1^2 \right]^{\frac{1}{2}} \tag{33}$$

To satisfy the condition of Equation (29),

$$A = \sqrt{3}$$

and the equivalent stress becomes

$$\sigma^* = \frac{1}{\sqrt{2}} \left[(\sigma_1 - \sigma_2)^2 + (\sigma_2 - \sigma_3)^2 + (\sigma_1 - \sigma_3)^2 \right]^{\frac{1}{2}} \tag{34}$$

A generalized plastic strain increment function is defined such that the product of the two is work.

$$dW^p = \sigma_{ij}\, d\varepsilon_{ij}^p \equiv \sigma^* d\varepsilon^* \tag{35}$$

After considerable manipulation,

$$d\varepsilon^* = \left\{ \frac{2}{3}\left[(d\varepsilon_1^p)^2 + (d\varepsilon_2^p)^2 + (d\varepsilon_3^p)^2 \right] \right\}^{\frac{1}{2}} \tag{36}$$

Inserting Equations (27) into Equation (36) and simplifying with Equation (34), it can be shown that

$$d\lambda = \frac{3}{2} \frac{d\varepsilon^*}{\sigma^*} \tag{37}$$

So that the stress-strain law now becomes

$$d\varepsilon_1^p = \left[\sigma_1 - \tfrac{1}{2}(\sigma_2 + \sigma_3) \right] \frac{d\varepsilon^*}{\sigma^*} \tag{38a}$$

$$d\varepsilon_2^p = \left[\sigma_2 - \tfrac{1}{2}(\sigma_1 + \sigma_3) \right] \frac{d\varepsilon^*}{\sigma^*} \tag{38b}$$

$$d\varepsilon_3^p = \left[\sigma_3 - \tfrac{1}{2}(\sigma_1 + \sigma_2) \right] \frac{d\varepsilon^*}{\sigma^*} \tag{38c}$$

Simplifying Equation (38a) to uniaxial tension, $d\varepsilon_1^p = d\varepsilon^*$ because $\sigma^* = \sigma_1$; thus, upon integration , $\varepsilon_1^p = \varepsilon^*$, since $\varepsilon^* = 0$ when $\varepsilon_1^p = \varepsilon_2^p = \varepsilon_3^p = 0$. This leads to a relationship between σ^* and ε^* .

It is postulated that if in uniaxial tension, for loading

$$\varepsilon_1^p = F(\sigma_1) \tag{39}$$

then a reasonable generalization is

$$\varepsilon^* = F(\sigma^*) \tag{40}$$

For instance, using the Ramburg-Osgood expression for uniaxial tensile behavior,

$$\varepsilon_1^P = \beta\left(\frac{\sigma_1}{E}\right)^n \tag{41}$$

then it is proposed that

$$\varepsilon^* = \beta\left(\frac{\sigma^*}{E}\right)^n \tag{42}$$

and

$$d\varepsilon^* = n\frac{\beta}{E}\left(\frac{\sigma^*}{E}\right)^{n-1} d\sigma^* \tag{43}$$

The stress-strain expression now has the form

$$d\varepsilon_1^P = \left[\sigma_1 - \tfrac{1}{2}(\sigma_2+\sigma_3)\right] n\frac{\beta}{E^2}\left(\frac{\sigma^*}{E}\right)^{n-2} d\sigma^* \tag{44}$$

For the notch specimens the loading was proportional; i.e.

$$\frac{\sigma_2}{\sigma_1} = \alpha_1 \qquad \frac{\sigma_3}{\sigma_1} = \alpha_2 \tag{45}$$

Under these conditions the plastic strain becomes

$$d\varepsilon_1^P = \gamma\sigma_1 n\frac{\beta}{E^2}\left(\frac{\sigma^*}{E}\right)^{n-2} d\sigma^* \tag{46}$$

where γ = Const = $1 - 1/2(\alpha_1 + \alpha_2)$.

Also generalized stress from Equation (34) becomes,

$$\sigma^* = \delta \sigma_1 \tag{47}$$

where δ = Const = $\frac{1}{\sqrt{2}} \left[(1-\alpha_1^2) + (\alpha_1 - \alpha_2)^2 + (1-\alpha_2^2) \right]^{\frac{1}{2}}$

Equation (46) then simplifies to

$$d\varepsilon_1^p = \delta^{n-1} \gamma n \frac{\beta}{E^n} \sigma_1^{n-1} d\sigma_1 \tag{48}$$

This is now integrable, and ε_1^p can be found explicitely.

$$\varepsilon_1^p = \delta^{n-1} \gamma \beta \left(\frac{\sigma_1}{E} \right)^n \tag{49}$$

The integration constant is zero from Equation (41).

Eliminating γ and δ using Equations (46) and (47), the plastic strain can be expressed in terms of stresses.

$$\varepsilon_1^p = \left[\sigma_1 - \tfrac{1}{2}(\sigma_2 + \sigma_3) \right] \frac{\beta}{E} \left(\frac{\sigma^*}{E} \right)^{n-1} \tag{50}$$

The elastic and plastic parts of the strain are assumed additive

$$\varepsilon_1 = \varepsilon_1^e + \varepsilon_1^p \tag{51}$$

and the total strain becomes

$$\varepsilon_1 = \frac{1}{E} \left[\sigma_1 - \nu(\sigma_2 + \sigma_3) \right] + \frac{\beta}{E} \left(\frac{\sigma^*}{E} \right)^{n-1} \left[\sigma_1 - \tfrac{1}{2}(\sigma_2 + \sigma_3) \right] \tag{52}$$

For plane stress, $\sigma_3 = 0$, and both of the other components can be obtained by permutation.

$$\varepsilon_1 = \frac{1}{E}\left[\sigma_1 - \nu\sigma_2\right] + \frac{\beta}{E}\left[\sigma_1^2 - \sigma_1\sigma_2 + \sigma_2^2\right]^{\frac{n-1}{2}}\left[\sigma_1 - \tfrac{1}{2}\sigma_2\right] \quad (53a)$$

$$\varepsilon_2 = \frac{1}{E}\left[\sigma_2 - \nu\sigma_1\right] + \frac{\beta}{E}\left[\sigma_1^2 - \sigma_1\sigma_2 + \sigma_2^2\right]^{\frac{n-1}{2}}\left[\sigma_2 - \tfrac{1}{2}\sigma_1\right] \quad (53b)$$

$$\varepsilon_3 = -\frac{\nu}{E}\left[\sigma_1 + \sigma_2\right] - \frac{\beta}{E}\left[\sigma_1^2 - \sigma_1\sigma_2 + \sigma_2^2\right]^{\frac{n-1}{2}}\left[\tfrac{1}{2}(\sigma_1 + \sigma_2)\right] \quad (53c)$$

This stress-strain law will be used to find stresses from photoelastic strain data, and all other analysis of the plastic zone around the notch except for the work done with the rigid - perfectly plastic model, which was used for the slip-line theory. Since the strains in the coating are constrained to be the same as the specimen, the equations relating strains and fringe will remain valid into the plastic domain. With ε_1 and ε_2 determined from the photoelastic data, a program for the solution of simultaneous, nonlinear, algebraic equations was used to solve Equations (53a) and (53b) for σ_1 and σ_2 . With σ_1 and σ_2 , ε_3 could be found from Equation (53c) if desired.

PLASTIC MEASUREMENTS AT THE NOTCH

The shallow notch specimen shown in Figure 2 was fabricated from 7075-T6 and loaded into the plastic range. Normal and oblique incidence fringes were recorded in 1/16" increments on the line of symmetry extending from the notch tip beginning at

1/8 inches and extending to 1/2 inches. Five different readings were taken at each location while the specimen was under 70,000 lbs. of load. The readings, along with the mean and the standard deviation, are recorded in Table III and Table IV.

With five samples taken, data falling outside of an expected value of 1/2n , or 1/10, were rejected. For a normal distribution this is $\pm 1.645\sigma$ from the mean. The data were examined for this tolerance and one oblique reading at x = .1875 in. fell outside the limits and was discarded. A new average was computed at this location of 7.71.

EXTRAPOLATION

A linear regression ignoring the sign was run for both sets of data using log (log N) vs. x as the function that is nearly linear. Results of the regression for normal incidence gave

$$\log (\log N) = .03627 - .2594x \qquad (54)$$

with R = .9997. At the edge of the hole, x = 0 , N = - 12.22. (The negative sign was again affixed after the value was found. For oblique incidence,

$$\log (\log N_\theta) = .01588 - .3566x \qquad (55)$$

with R = .9984. At the edge of the hole , N_θ = - 10.895.

POISSON'S RATIO MISMATCH

This extrapolation was made from a region of the sheet where the Poisson's Ratio of the metal is 0.5 due to yielding. From Lindsey[4] the effective Poisson's Ratio in the coating material is given by

TABLE III FRINGE VALUES

SHALLOW NOTCH TEST - NORMAL INCIDENCE - PLASTIC LOAD

x	1	2	3	4	5	AUG	S.D.
.5000	6.36	6.39	6.40	6.42	6.39	6.392	.0217
.4375	6.83	6.83	6.85	6.87	6.84	6.844	.0167
.3750	7.44	7.44	7.41	7.41	7.42	7.424	.0152
.3125	7.98	7.99	8.03	8.08	8.06	8.028	.0432
.2500	8.65	8.64	8.65	8.67	8.67	8.656	.0134
.1875	9.29	9.33	9.38	9.37	9.35	9.344	.0358
.1250	10.11	10.20	10.19	10.16	10.23	10.177	.0455

TABLE IV FRINGE VALUES

SHALLOW NOTCH TEST - OBLIQUE INCIDENCE - PLASTIC LOAD

x	1	2	3	4	5	AUG	S.D.
.500	4.79	4.79	4.79	4.79	4.79	4.790	0
.4375	5.41	5.39	5.36	5.32	5.32	5.360	.0406
.3750	5.85	5.85	5.84	5.84	5.86	5.848	.0084
.3125	6.41	6.40	6.41	6.40	6.37	6.398	.0164
.2500	7.06	6.97	7.03	6.89	6.97	6.984	.0654
.1875	7.79	7.70	7.71	7.73	7.70	7.726	.0378
.1250	0.62	8.57	8.55	8.58	8.58	8.58	.0255

$$\bar{\nu} = \frac{.4797 - .1207\left[\dfrac{\cosh\left(\frac{\pi x^*}{2h_c}\right)}{\cosh(5\pi)}\right]}{.9923 - .0458\left[\dfrac{\cosh\left(\frac{\pi x^*}{2h_c}\right)}{\cosh(5\pi)}\right]} \qquad (56)$$

Where x* is measured from an interior point far from the edge of the coating. To relate it to x which is measured inward from the notch edge, let $x^* = 10\ h_c - x$. For photoelastic measurements at points where $x \geq .1250$ in, Poisson's Ratio is essentially constant. The coating being used was hc = .0382 ;thus x = .1250 corresponds to $x = 3.2723h_c$ and $x^* = 6.7277h_c$. Substituting this value into (56) gives $\bar{\nu} = .4828$.

However when extrapolating back to x = 0 , the extrapolation is from data for which the value of $\bar{\nu}$ is .4828 but the actual value there from (56) is .3793. Lindsey[4] worked out the correction for the extrapolation:

$$[N]_{\bar{\nu}=.3793} = \left(\frac{1+.3793}{1+.4828}\right)[N]_{\bar{\nu}=.4828} \qquad (57)$$

The same correction applies to the oblique incidence fringes; therefore, the fringe value at the edge of the notch is

$$N = (.9302)(-12.22) = -11.37 \qquad N_\theta = (.9302)(-10.90) = -10.13 \qquad (58)$$

REINFORCEMENT

A slight reinforcement of the thin metal sheet by the coating material is present, and this small correction factor was developed in Part I.

$$\varepsilon_1^u - \varepsilon_2^u = \left[1 + \frac{h_c E_c (1+\nu_s)}{h_s E_s (1+\nu_c)}\right](\varepsilon_{1c} - \varepsilon_{2c}) \qquad (59)$$

In the elastic domain, the factor was 1.0162, but in the plastic domain it is 1.0182. This correction only need be made if comparisons are being made with calculations or measurements being made on an uncoated part, and this will be the case when comparisons are made later with finite element solutions. The finally corrected values of the fringes are given in Table V.

STRAINS

The strain expressions reflecting the calibrated parameters of the polariscope in the Aeronautical Engineering laboratory at NPS are[4]

$$\varepsilon_x = \frac{-F_\varepsilon}{(1+\bar{\nu})}\left[(2.6012-3.6012\bar{\nu})N - 3.0607(1-\bar{\nu})N_\theta\right] \tag{60a}$$

$$\varepsilon_y = \frac{-F_\varepsilon}{(1+\bar{\nu})}\left[(3.6012-2.6012\bar{\nu})N - 3.0607(1-\bar{\nu})N_\theta\right] \tag{60b}$$

where $\varepsilon_x - \varepsilon_y = F_\varepsilon N$ and ε_x may or may not be the larger principal strain. At the edge of the hole where $\bar{\nu} = .3793$

$$\varepsilon_x^u = -1.5798\times10^{-3}N + 2.4296\times10^{-3}N_\theta \tag{61a}$$

$$\varepsilon_y^u = -3.3438\times10^{-3}N + 2.4296\times10^{-3}N_\theta \tag{61b}$$

At the next station and all remaining stations, $x \geq 0.1250$in., Poisson's Ratio is 0.4828 and the strain expressions are given by

$$\varepsilon_x^u = -1.0261\times10^{-3}N + 1.8832\times10^{-3}N_\theta \tag{62a}$$

$$\varepsilon_y^u = -2.7901\times10^{-3}N + 1.8832\times10^{-3}N_\theta \tag{62b}$$

TABLE V CORRECTED FRINGE VALUES

x	N	N_θ
0.0000	- 11.58	- 10.31
.1250	- 10.36	- 8.74
.1875	- 9.51	- 7.85
.2500	- 8.81	- 7.11
.3125	- 8.17	- 6.51
.3750	- 7.56	- 5.95
.4375	- 6.97	- 5.46
.5000	- 6.51	- 4.88

Using the fringe values of Table V in Equations (61) and (62), the strain distribution is obtained in Table VI.

STRESSES

The nonlinear constitutive relations developed in Equations (53a) and 53b) were used to find stresses. Since the equations cannot be solved explicitly for stress, a computer program was used to solve the nonlinear set of equations simultaneously. Results in the form of a stress distribution are given in Table VII, where the following values of the parameters were used as given by Lindsey[2] in Part II.

$E = 10.12 \times 10^6$ psi

$\nu = 0.5$

$\beta = 1.479 \times 10^{43}$

$n = 21.58$

The σ_x value at $x = 0$ should be zero of course; however it is less than 1% of the other stress component and represents a small experimental error. To continue the investigation of the plastic region at the notch, a finite element analysis was conducted to be used in conjunction with the photoelastic results.

FINITE ELEMENT ANALYSIS

The ADINA Program was used as described in Part II. The grids for the notch are shown in Figures 8 and 9. The analysis for loading into the plastic region of the 7075-T6 aluminum was made using a bilinear material model mentioned earlier. The values required by ADINA were determined graphically from experimental data shown in Figure 10 and the bilinear fit is also

TABLE VI PLASTIC STRAIN DISTRIBUTION

x	$\varepsilon_x \times 10^3$	$\varepsilon_y \times 10^2$
0.0	- 6.7551	1.3672
0.1250	- 5.8288	1.2446
0.1875	- 5.0249	1.1751
0.2500	- 4.3496	1.1191
0.3125	- 3.8764	1.0535
0.3750	- 3.4477	.9888
0.4375	- 3.1304	.9165
0.5000	- 2.5101	.8974

TABLE VII STRESS DISTRIBUTION

x	σ_x (psi)	σ_y (psi)
0	629	79,945
.1250	3,327	80,441
.1875	7,533	81,813
.2500	11,466	82,975
.3125	13,447	83,102
.3750	15,214	83,012
.4375	15,696	82,145
.5000	21,474	83,847

FIGURE 8 COURSE MESH FOR SHALLOW NOTCH

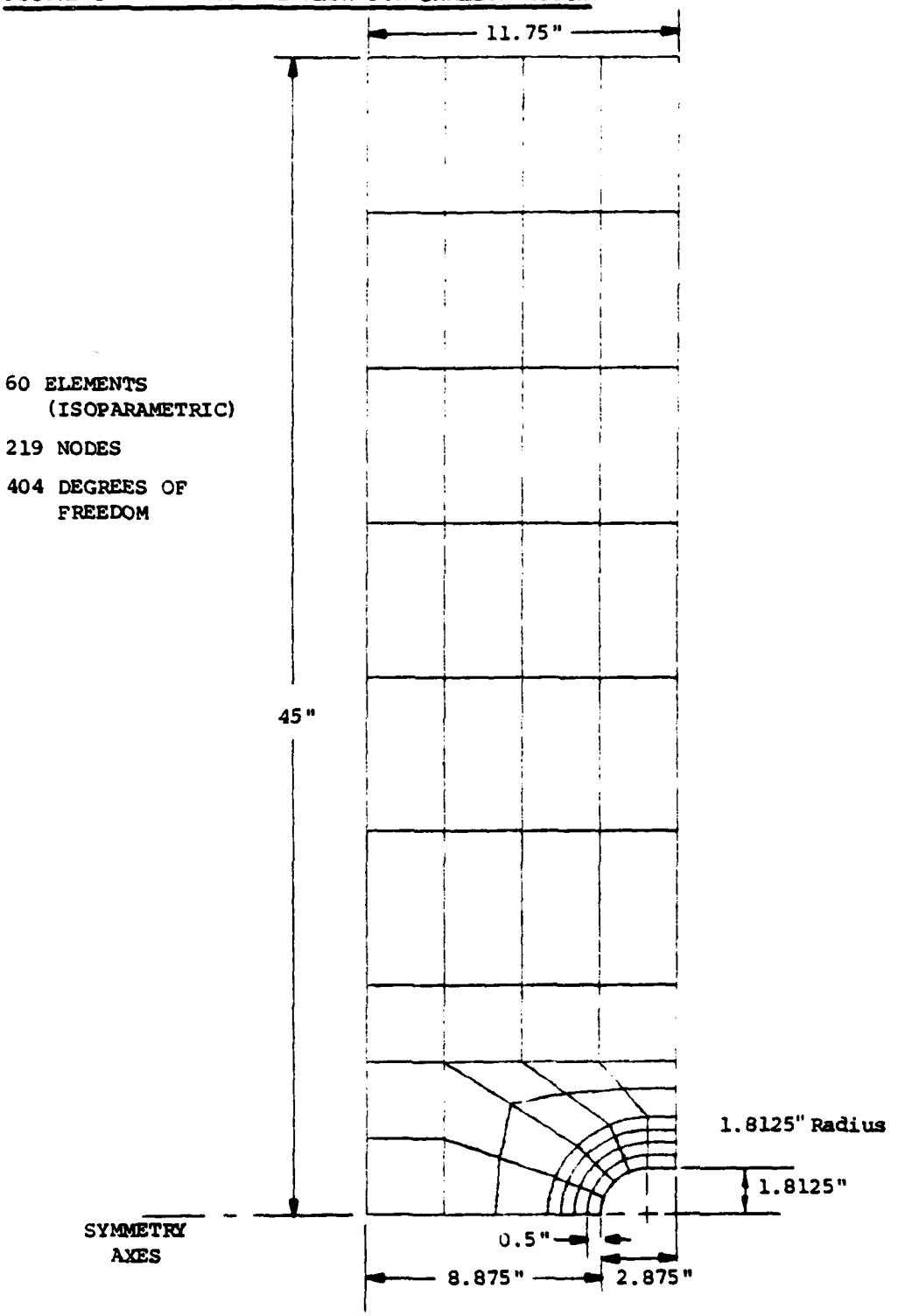

FIGURE 9 FINE MESH FOR SHALLOW NOTCH

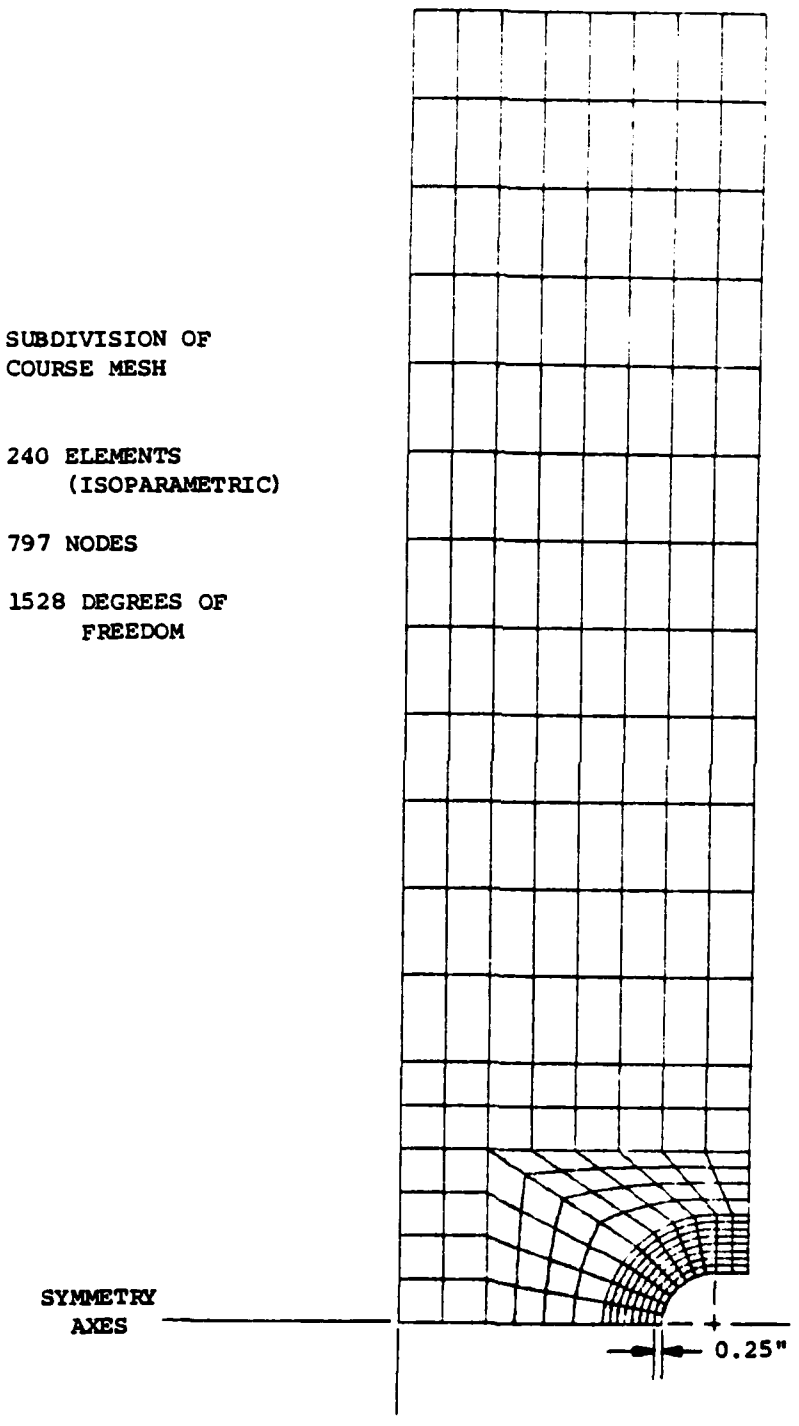

FIGURE 10

7075-T6 ALUMINUM STRESS-STRAIN CURVE

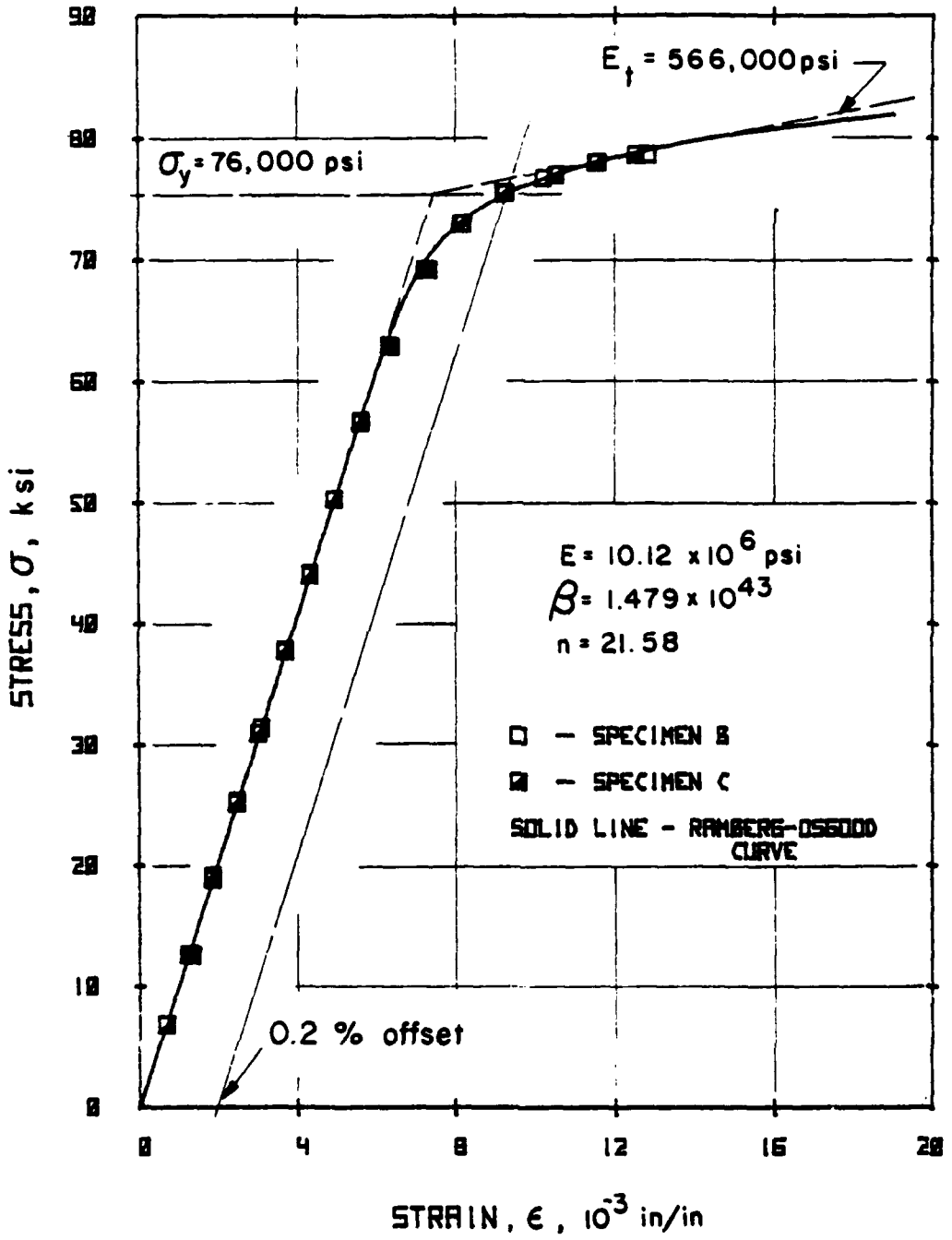

shown. The loads used in the program were selected to match the experiments.

The results of FEA for a local yield producing load of 70,000 lbs are presented along with the experimental results in Figure 11. The σ_θ results compare well, matching in both magnitude and trend with the experimental data. In all cases the FEA determined the peak σ_θ stress to occur near the yield boundary, and the gradient of the σ_r stress to fall off dramatically in the plastic zone. This characteristic behavior of the σ_θ stress was reported by other investigators [References 5 and 6] using FEA on 2024-T3 aluminum. Plane elastic-plastic stress distributions reported by Frocht [Reference 7] show similar trends. The experimental data also shows a marked change in the gradient of σ_θ stress within the plastic region. The growth of this plastic region is approximated by using the FEA results for this notch loaded at 60,000, 65,000 and 70,000 lbs. These results are shown in Figures 12 through 14. Experimental data for the σ_θ stress distribution matches the FEA results reasonably close.

The compatibility of the data is satisfying because the finite element mesh cannot be made too fine without becoming unwieldly, while the photoelastic data is continuous. Also because of the averaging techniques used to extrapolate the finite element results, the stress values in regions of high gradients are suspect. On the other hand, the finite element

FIGURE 11

SHALLOW NOTCH 70000 LB LOAD ELASTIC-PLASTIC RESULTS

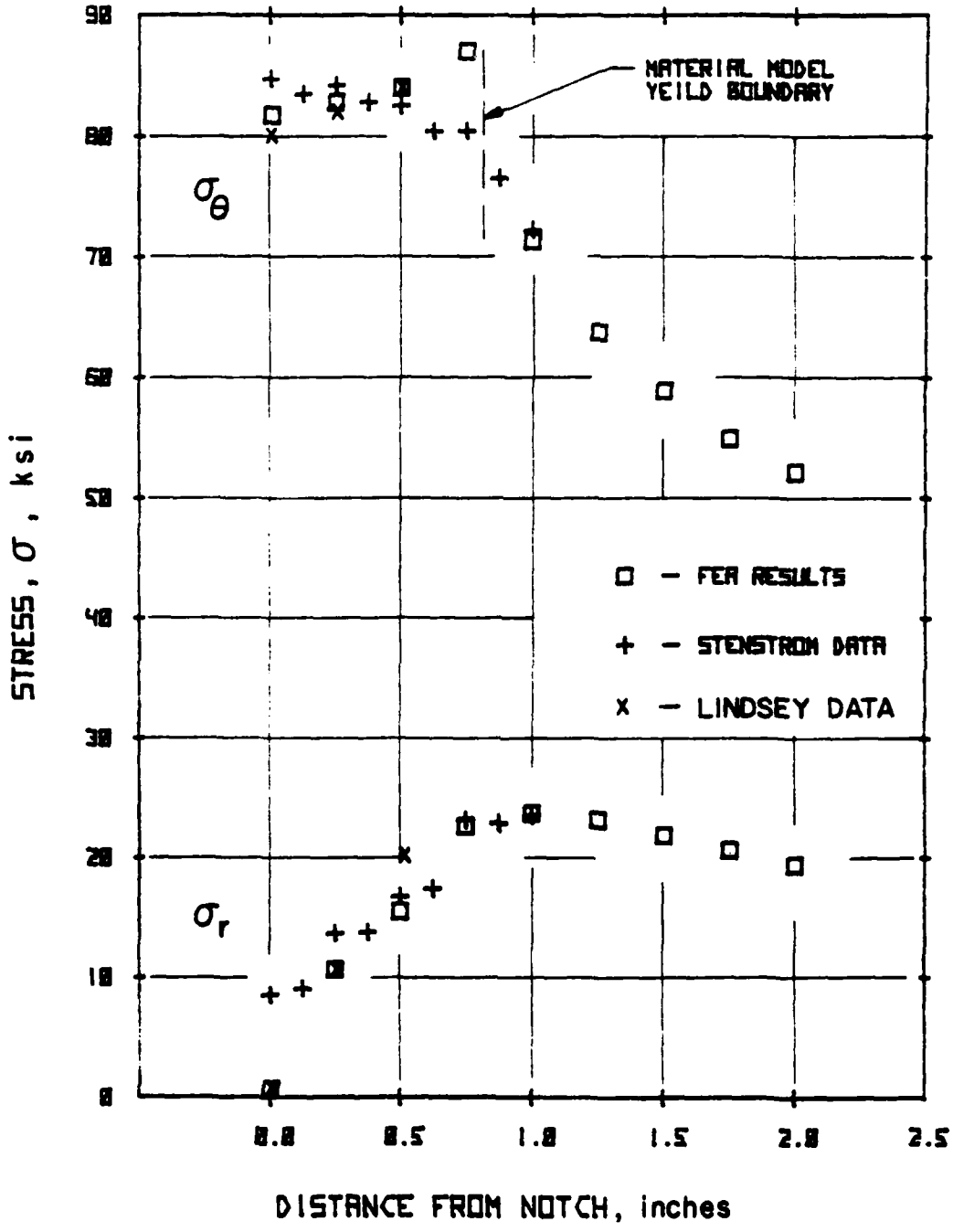

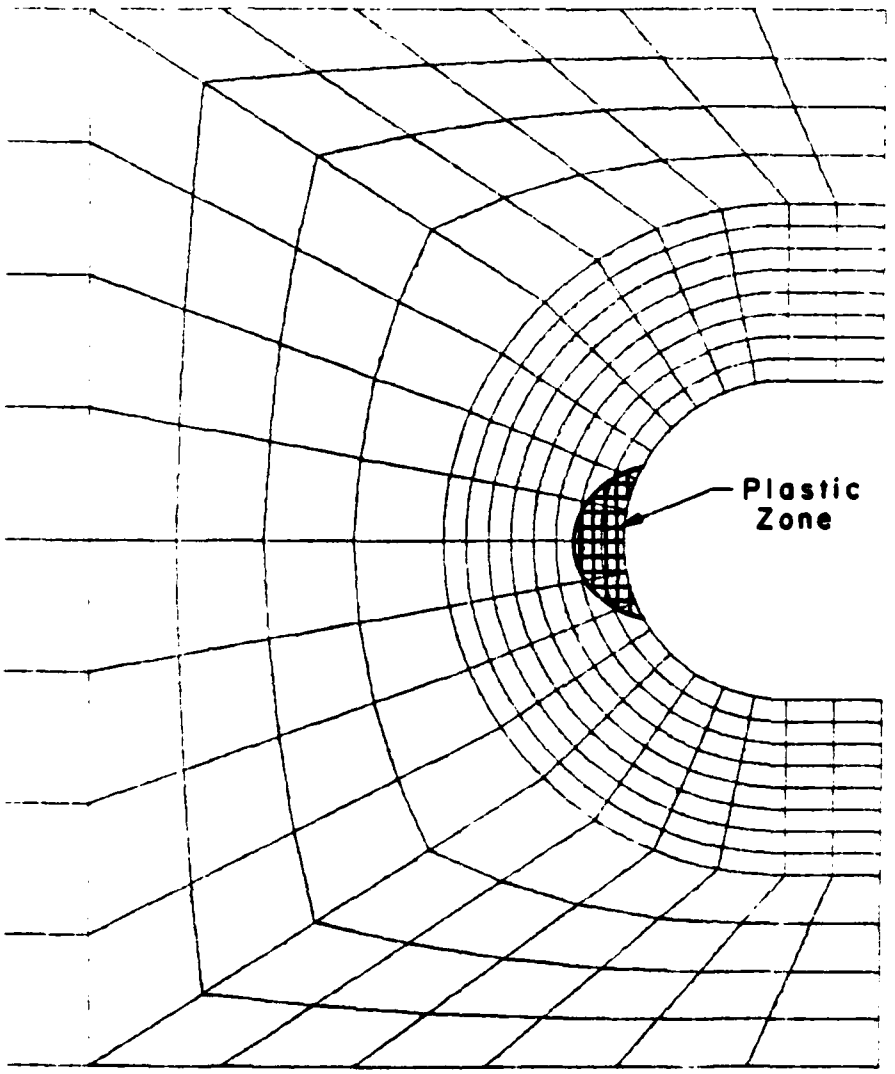

FIGURE 12

SHALLOW NOTCH 60,000 LB LOAD PLASTIC ZONE

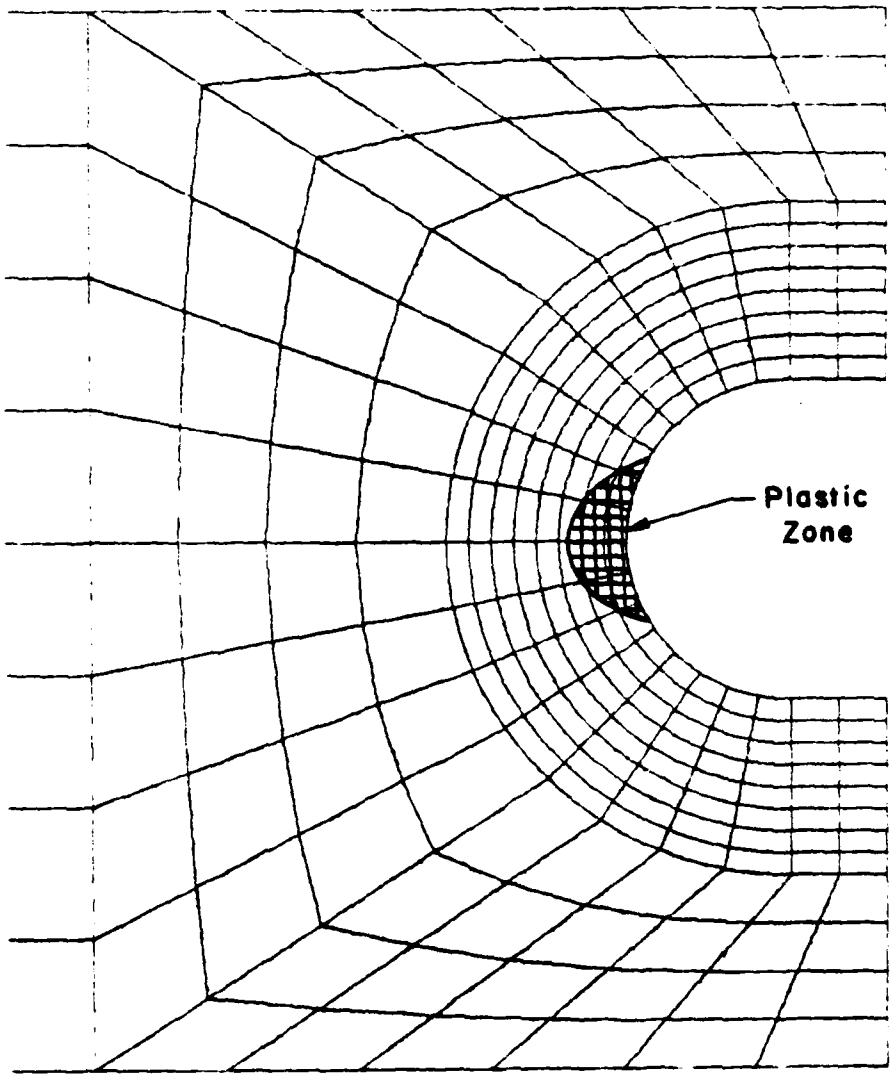

FIGURE 13

SHALLOW NOTCH 65,000 LB LOAD PLASTIC ZONE

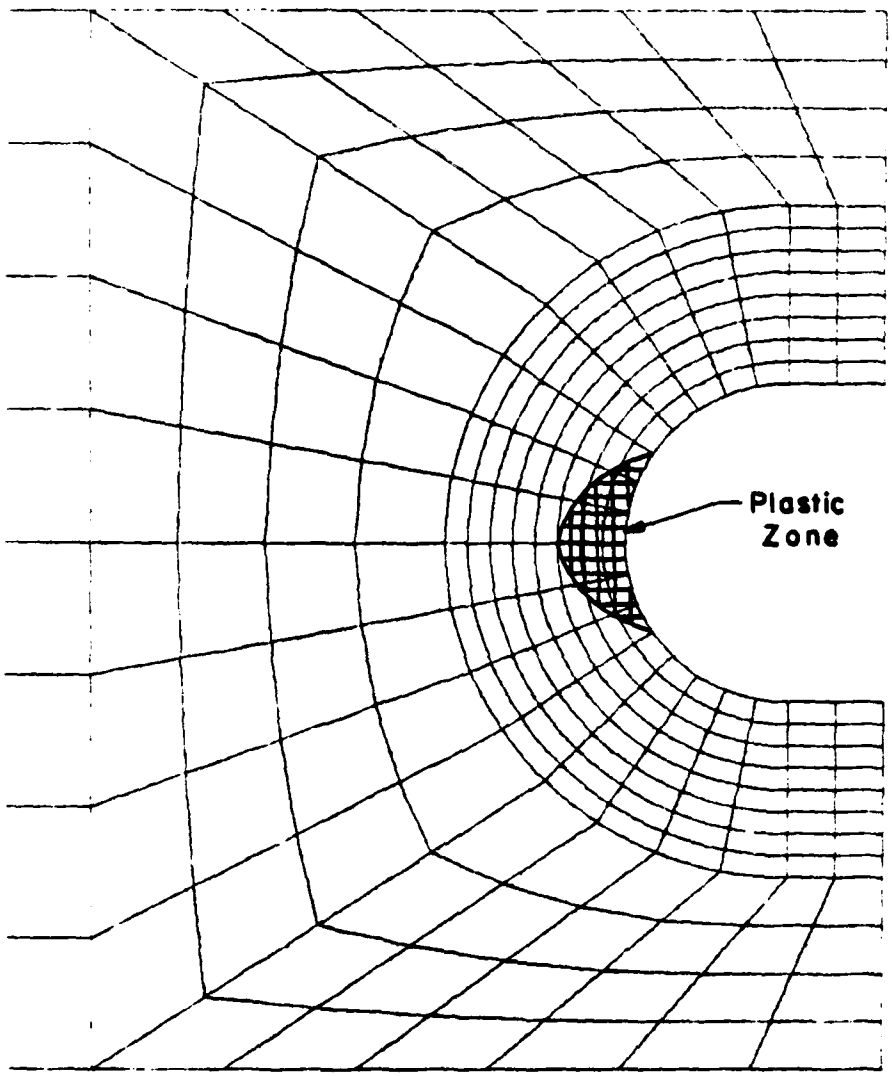

FIGURE 14

SHALLOW NOTCH 70,000 LB LOAD PLASTIC ZONE

solution is readily obtained over the whole elastic-plastic region and that would be very laborious using photoelascity by running them both, reliable results seem to be reasonably certain.

STRESS AND STRAIN CONCENTRATION FACTORS

Turning attention to the notch boundary only, a development is made whereby the local hoop stress can be calculated. In the elastic range, stress and hoop stress can be calculated. values to nominal values are constant and equal.

$$K_\sigma = K_\varepsilon = K_T$$

In this definition the stress concentration factor was defined as local stress over smallest cross-section stress. In the yielded domain, these elastic relationships change, K_σ and K_ε are no longer equal and their values depend upon the amount of plastic yielding that takes place at the notch-tip.

LOADING INTO THE PLASTIC RANGE

To show these relationships, Figure 15a has been constructed. It is for a most general case showing local conditions versus far-field conditions of both stress and strain. The stress-strain curve which corresponds to the loading cycle in Figure 15a is shown in Figure 15b with all corresponding points labeled the same.

Loading begins at 1 with yielding occurring at 2; so from 1 to 2,

$$\sigma = K_\sigma S = K_T S \tag{63}$$

$$\dot{\varepsilon} = K_\varepsilon e = K_T e \tag{64}$$

Loading continues to point 4 where unloading begins and the cycle is completed at point 5, where there is positive residual strain and negative residual stress.

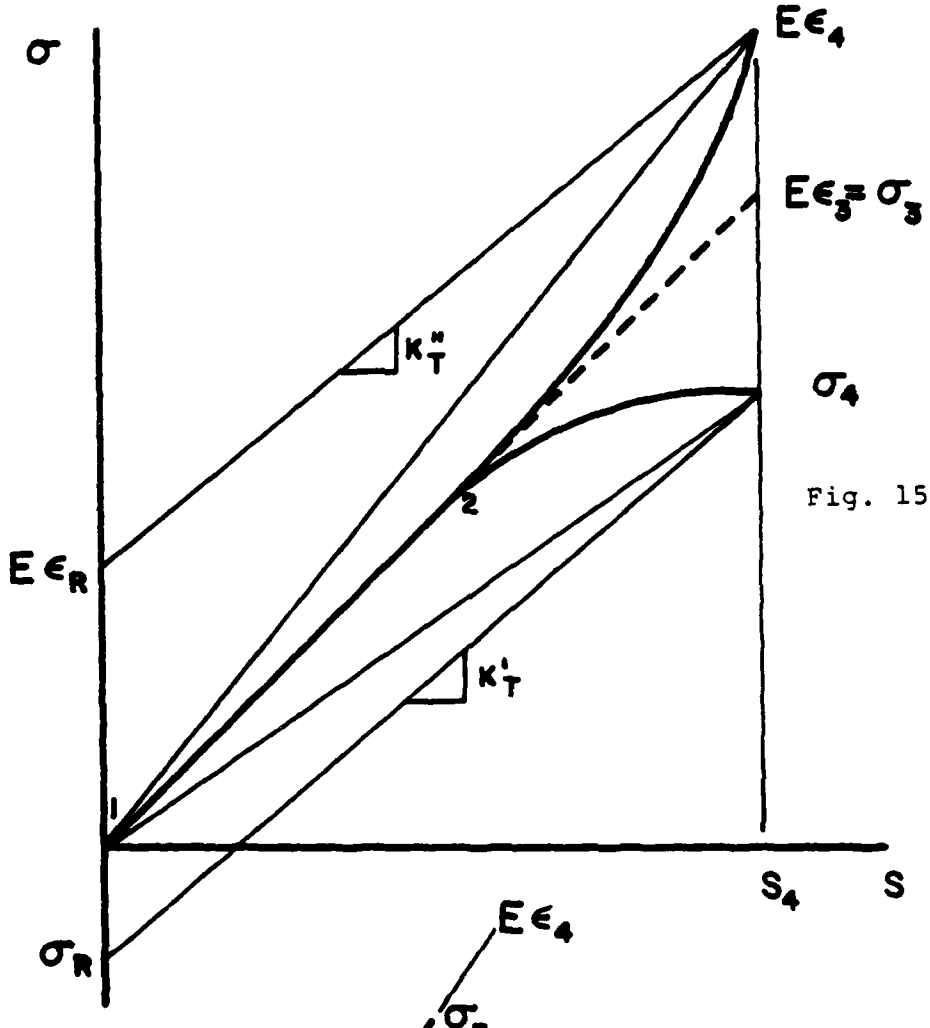

Fig. 15a Stress - Stress Diagram

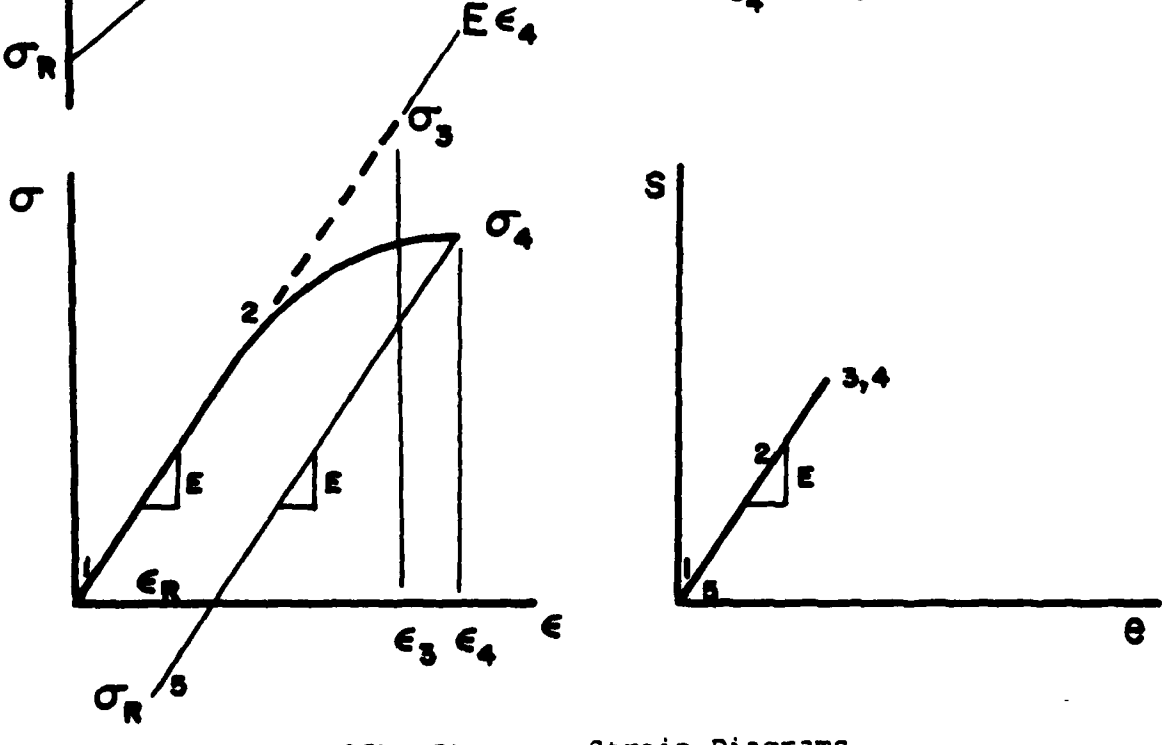

Fig. 15b Stress - Strain Diagrams

UNLOADING

During unloading, and for subsequent loading cycles up to yield, the stress concentration factor is elastic and constant, but different from the original K_T. This is shown in Figure 15a.

$$K_T' = \frac{\sigma_4 - \sigma_R}{S_4} \tag{65}$$

Since $K_\sigma = \sigma_4 / S_4$,

$$K_T' = K_\sigma - \frac{\sigma_R}{S_4} \tag{66}$$

During the same portion of the cycle the unloading strain concentration factor from Figure 15a is

$$K_T'' = \frac{\varepsilon_4 - \varepsilon_R}{e_4} \tag{67}$$

Since $K_\varepsilon = \varepsilon_4 / e_4$, and $S_4 = E e_4$,

$$K_T'' = K_\varepsilon - \frac{E \varepsilon_R}{S_4} \tag{68}$$

From Figure 15b,

$$\sigma_4 - \sigma_R = E(\varepsilon_4 - \varepsilon_R) \tag{69}$$

Solving for σ_R and inserting it into Equation (65)

$$K_T' = K_\sigma - \frac{\sigma_4}{S_4} + \frac{E}{S_4}(\varepsilon_4 - \varepsilon_R) \tag{70}$$

Simplifying by summing the first two terms to zero and using the elastic relation $S_4 = e_4$,

$$K_T' = K_\varepsilon - \frac{E\varepsilon_R}{S_4} \tag{71}$$

Comparing equation (71) with equation (68)

$$K_T' = K_T'' \tag{72}$$

This result for the uniaxial model has some rather far-reaching implications. One of them is that the strain concentration factor is the same as the elastic stress concentration factor even into the plastic domain. This is shown by returning to equation (71). From Figure 15a for parallel unloading curves of stress and strain,

$$E\varepsilon_R - \sigma_R = E\varepsilon_4 - \sigma_4 \tag{73}$$

Solving for $E\varepsilon_R$ and inserting it into (71)

$$K_T' = K_\varepsilon - \frac{(\sigma_R - \sigma_4 + E\varepsilon_4)}{S_4} \tag{74}$$

Since $\frac{E\varepsilon_4}{S_4} = K_T$ and $\frac{\sigma_4 - \sigma_R}{S_4} = K_T'$, equation (74) reduces to

$$K_\varepsilon = K_T \tag{75}$$

which establishes K_ε in the plastic region to be a constant. This is a very important result which can be checked experimentally.

Inserting expressions of stress and strain into (75)

$$\frac{\varepsilon_4}{e_4} = \frac{E\varepsilon_4}{S_4} = \frac{\sigma_3}{S_4} \tag{76}$$

Since σ_3 is an elastic value and related to ε_3 through Young's modulus, we may conclude

$$\varepsilon_3 = \varepsilon_4 \tag{77}$$

This simplification, with the others already noted reduces Figure 15 to that appearing in Figure 16. In the second application of load, $K_\varepsilon = K_T'$ and $K_\sigma = K_T'$ until the previous highest stress and strain values are exceeded.

RELATING LOCAL STRESS TO FAR-FIELD STRESS

After yielding has taken place, we desire to relate K_σ to K_T so that local stresses can be readily found at the notch from a knowledge of the loading and K_T . From the uniaxial stress-strain expression, which governs the ligament at the tip of the notch,

$$\varepsilon = \frac{\sigma}{E} + \beta\left(\frac{\sigma}{E}\right)^n \tag{78}$$

We have shown that

$$\varepsilon = K_\varepsilon e = K_T e \tag{79}$$

Putting Equation (78) into Equation (79), K_T can be related to the local stress at the notch-tip.

$$K_T = \frac{\sigma}{Ee} + \frac{\beta\sigma}{Ee}\left(\frac{\sigma}{E}\right)^{n-1} \tag{80}$$

In the plastic domain,

$$S = Ee \qquad K_\sigma = \frac{\sigma}{S} \tag{81}$$

Equation (86) can be written in terms of stress concentration factors to show the relationship after yielding.

$$K_T = K_\sigma \left[1 + \beta \left(\frac{\sigma}{E} \right)^{n-1} \right] \tag{82}$$

This is a competitor to Neuber's Relation, which has been used by many to calculate local stresses at notches that are yielded. A comparison of the accuracy of this equation compared with Neuber's relation will be made later.

RESIDUAL STRESS

For each point along the loading curve in the plastic range, if unloading occurred at that point

$$K_T' = \frac{\sigma - \sigma_R}{S} \tag{83}$$

which relates the modified elastic SCF to the plastic one. From Equation (65),

$$K_T' = K_\sigma - \frac{\sigma_R}{S} \tag{84}$$

This SCF will be valid until the next load cycle that will cause additional yielding is applied.

As the unloading continues, an unloaded equilibrium point will be reached with a positive residual strain and a negative residual stress. The value of the coordinates in stress-strain space where this will occur cannot be calculated with this model. If the residual strain is measured photoelastically, the residual stress can be calculated from Equation (65). The new stress concentration factor can be checked photoelastically. All of this has been done.

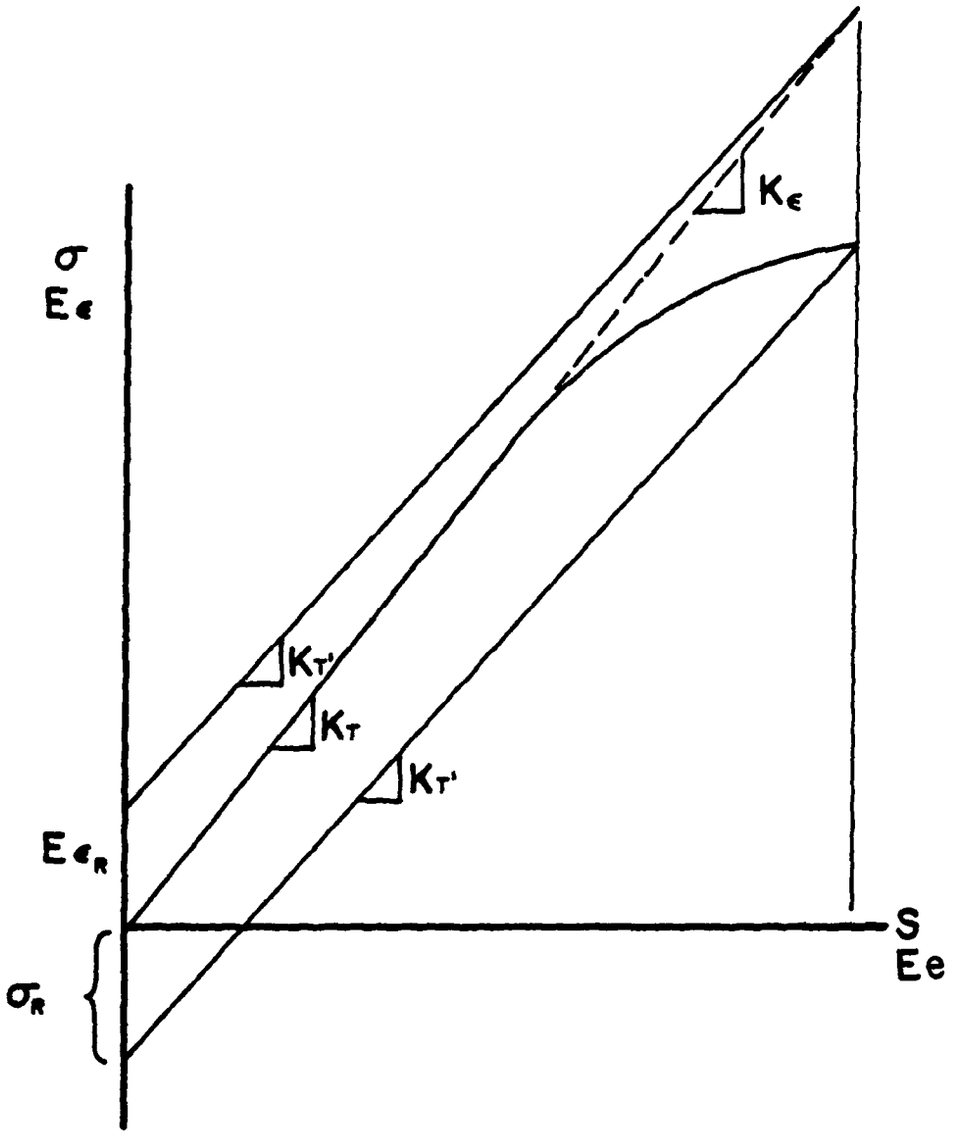

Figure 16. Derived Stress - Strain Diagram

CHECK OF THE THEORY

A 70,000 lb. load was applied to the notched specimen of Figure 2, which has a nominal cross-sectional area of 1.42 in^2. The nominal stress is S = 49,296 psi, and the nominal strain is $e = 4.8711 \times 10^{-3}$ in/in ($E = 10.12 \times 10^6$ psi). By a previous development it was shown that even for strains into the plastic range, which this loading does produce for the material at the notch tip, the strain concentration factor does not change.

$$\varepsilon = K_T e = (2.73)(4,8711 \times 10^{-3}) = .0133 \text{ in/in}$$

Normal incidence photoelastic measurements at the notch made by Stenstrom [8] are recorded in Table VII. Extrapolating to zero as described in Part I gives a compensator reading of $C_n = 545.2$, or a fringe value of 11.6. Reinforcement effects of the coating amount to a factor of 1.0182 when the material is yielded, and the Poisson's Ratio mismatch produces a factor of .9195. The actual fringe value is the product of the three, or 10.86. From the photoelastic fringe equation.

$$\varepsilon_1 - \varepsilon_2 = (1796 \times 10^{-6})\ (10.86) = 0.01950 \text{ in/in}$$

At the notch tip we are assuming a uniaxial stress which requires that $\varepsilon_2 = -\nu\varepsilon_1$ where $\nu = 0.5$; thus

$$\varepsilon_1 = 0.0130 \text{ in/in}$$

TABLE VII STENSTROM DATA

PLASTIC REGION LOADING

K_T = 2.6 Notch, 70,000 lb. Load

Data Pt. In.	Corrected C_n	Corrected C_θ	ε_1 10^{-3}in/in	ε_2 10^{-3}in/in	σ_1 psi	σ_2 psi
0.0	571.0	678.0	16.182	-5.244	163866	800
0.125	464.4	545.8	13.410	-4.014	137050	4426
0.250	393.9	472.4	11.960	-2.819	125057	12570
0.375	339.7	410.1	10.480	-2.264	110367	13360
0.500	294.5	361.8	9.476	-1.576	101522	17420
0.625	253.3	314.6	8.362	-1.143	90502	18160
0.750	219.1	281.4	7.807	-0.415	86927	24360
0.875	193.0	250.3	7.027	-0.215	78828	23710
1.000	170.9	225.3	6.436	0.024	73027	24220
RESIDUAL COMPRESSION						
0.0	178.0	211.0	-5.025	1.654	-50791	43
0.125	158.8	185.8	-4.535	1.424	-46086	-736
0.250	139.7	163.7	-4.004	1.238	-40774	-878
0.375	117.6	138.1	-3.389	1.023	-34600	-1016
0.500	100.5	118.5	-2.926	0.845	-30017	-1316
0.625	81.4	96.5	-2.402	0.652	-24798	-1551

This is a favorable comparison confirming the uniaxial model and the development of the constancy of the strain concentration factor. The error is 2.25%.

The maximum stress is calculated from

$$\varepsilon_1 = \frac{\sigma_1}{10.12 \times 10^6} + 1.479 \times 10^{43} \left(\frac{\sigma}{10.12 \times 10^6} \right)^{21.58}$$

Obtaining the value numerically, the maximum stress is 79,403 psi. The small error in strain is insignificant when stresses are calculated. This could have been calculated directly from the loading by using Equation (78).

The residual strain was measured after a maximum load of 71,000 lb. had been applied. Extrapolation to the notch tip gave $N_R = 2.91$, which determines the residual strain at 3.48×10^{-3} in/in. The associated residual stress is obtained from the model by Figure 15b

$$\sigma_R = E(\varepsilon_R - \varepsilon_{Ro})$$

where $\varepsilon_{Ro} = \varepsilon_4 - \frac{\sigma_4}{E}$

For this load $\varepsilon_4 = 0.0135$ and $\sigma_4 = 79,529$ psi,
These values give $\varepsilon_{Ro} = 5.6414 \times 10^{-3}$ in/in, and $\sigma_R = -21,873$ psi.

From Equation (65) the new SCF for the next loading cycle is $K_T^1 = 2.03$. An elastic reloading was made with photoelastic measurements taken at the notch to evaluate the new K_T^1. A 20,000 lb. load was applied which gave a local strain reading of

6.368×10^{-3} in/in, which produced a strain rise from the residual value of 2.888×10^{-3} in/in and an associated stress rise of 29,228 psi. The nominal stress was 20,000 lb. acting over 1.42 in^2 , and the new SCF was 2.08 as compared to a predicted value of 2.03, which is a 2.4% error. Several other specimens were checked which resulted in predictions of similar accuracy. The actual stress state for the above example is 29,228 - 21,873 = 7355 psi. This is a significant influence on the fatigue life calculation.

SUMMARY AND CONCLUSIONS

A two-dimensional plasticity stress-strain law has been developed to coordinate with the photoelastic measurements for performing nonlinear, plastic analysis of stress distributions around notches. These were compared to analytical solutions obtained by slipline theory for perfectly plastic materials.

A one-dimensional model of the stress field at the notch-tip has been used to successfully predict behavior there. Predictions have been verified by experimental measurements using photoelasticity.

The only remaining piece to be developed to have all the theory in place for fatigue applications is the one for calculation of residual stresses. All attempts at this so far have been unsuccessful.

REFERENCES

1. L. M. Kachanov, Foundation of the Theory of Plasticity, North Holland Publishing Co., Amsterdam, Holland, 1971.
2. G. H. Lindsey, "A Study of Notch Fatigue Part II: Elastic Stress Analysis of Notches". Report No. NPS67-81-005, Naval Postgraduate School, Monterey, California, 1981.
3. D. C. Drucker, "A Definition of Stable Inelastic Materials," Journal of Applied Mechanics, Vol. 26, Trans. ASME, Vol. 81, Series E, 1959, p.101.
4. G. H. Lindsey, "A Study of Notch Fatigue Part I: Static Photoelastic Measurements," Report No. NPS67-81-004, Naval Postgraduate School, Monterey, California, 1981.
5. National Aeronautics and Space Administration (NASA) Report CR-1649, Finite Element Analysis of Structures in the Plastic Range, by H. Armen, Jr., A. Pifko, and H. S. Levine, February, 1971.
6. Naval Research Laboratory Report 7278, Finite Element Analysis of Notched Tensile Specimens in Plane Stress, by C. A. Griffis, 10 September 1971.
7. Frocht, M. M., and Thomson, R. A., "Further Work on Plane Elastoplastic Stress Distributions," Proceedings of the International Symposium on Photoplasticity, Pergamon Press, Press, 1963.

INITIAL DISTRIBUTION LIST

		No. of Copies
1.	Defense Technical Information Center ATTN: DDC-TCA Cameron Station, Bldg. 5 Alexandria, VA 22314	2
2.	Library, Code 0212	2
	Dean of Research, Code 012 Naval Postgraduate School Monterey, CA 93940	1
3.	Chairman of Aeronautics Code 67 Naval Postgraduate School Monterey, CA 93940 Prof. M. F. Platzer, Chairman	1
4.	Dr. Dan Mulville Code 320B Naval Air Systems Command Washington, DC 20361	2
5.	Professor G. H. Lindsey Code 67Li Department of Aeronautics Naval Postgraduate School Monterey, CA 93940	2